

CALCIUM INWARD CURRENTS IN INTERNALLY PERFUSED GIANT AXONS

BY H. MEVES AND W. VOGEL

*From the Laboratory of the Marine Biological Association,
Plymouth and Physiologisches Institut,
Kiel, Germany*

(Received 29 May 1973)

SUMMARY

1. Voltage clamp experiments were carried out on squid axons perfused with an isotonic solution of 25 mM-CsF + sucrose and placed in a Na-free solution of 100 mM-CaCl₂ + sucrose.

2. Depolarizing voltage steps produced inward currents of 4–6 $\mu\text{A}/\text{cm}^2$ peak amplitude which decayed slightly during a 60 msec pulse; the inward current disappeared when the internal potential reached +50 to +60 mV and became outward for larger depolarizations.

3. Tetrodotoxin completely blocked the inward current and part of the outward current. No inward currents were seen with 100 mM-MgCl₂ + sucrose as the external solution. Substituting acetate for external Cl⁻ did not abolish the tetrodotoxin-sensitive outward currents.

4. It is concluded that the inward current is carried by Ca and the tetrodotoxin-sensitive outward current by Cs ions, both moving through the Na channel.

5. The reversal potential of the tetrodotoxin-sensitive current was in the average +54 mV. Raising the external Ca concentration or adding NaCl to the external solution increased the reversal potential; lowering the external Ca concentration or replacing the internal CsF by a Na salt decreased the reversal potential.

6. From the reversal potentials of the tetrodotoxin-sensitive current measured with varying external and internal solutions the relative permeabilities of the Na channel were calculated as $P_{\text{Ca}}/P_{\text{Cs}} = 1/0.6$, $P_{\text{Ca}}/P_{\text{Na}} = 1/10$ to $1/7$ and $P_{\text{Cs}}/P_{\text{Na}} = 1/22$ to $1/9$ by means of the constant field equation. The permeability ratios suggest that under these experimental conditions the Na channel is still primarily permeable to Na ions, although its selectivity is relatively small.

7. The time course of the tetrodotoxin-sensitive Ca inward current was different from the time course of the Na inward current. The Na current

consisted of an initial peak followed by a more slowly decaying component, the Ca current showed only the slow component.

8. The slowly inactivating tetrodotoxin-sensitive Ca inward currents give rise to the long lasting action potentials which have first been observed by Tasaki and coworkers under similar conditions.

INTRODUCTION

Calcium ions enter the squid axon during an action potential as has been shown with radioactive Ca (Hodgkin & Keynes, 1957; Tasaki, Watanabe & Lerman, 1967) and with aequorin as Ca indicator (Baker, Hodgkin & Ridgway, 1971). Voltage clamp experiments on aequorin injected fibres indicated that the Ca entry associated with a depolarizing pulse can be divided into two components, an early component which is blocked by tetrodotoxin and represents a leak of calcium ions through the Na channel and a late component which is not affected by tetrodotoxin.

The amount of Ca entering the fibre is very small. With 112 mM-Ca in the external solution the Ca entry measured with the tracer technique is in the order of 0.08 p-mole/cm² per action potential (Hodgkin & Keynes, 1957), corresponding to an electric charge of less than 0.02 $\mu\text{C}/\text{cm}^2$. This is small compared with the net Na entry of 3-4 p-mole/cm² which represents a charge transfer of 0.3-0.4 $\mu\text{C}/\text{cm}^2$.

One can envisage experimental conditions under which the small Ca entry which occurs upon depolarization might be sufficient to elicit an action potential. These conditions are (1) slow inactivation of the Ca inward current which would allow this weak current to flow for a sufficient time, (2) complete or nearly complete absence of outward current through the Na channel, the delayed channel or the leakage channel. The two conditions are ideally fulfilled in axons internally perfused with a non-electrolyte solution containing a small amount of CsF. In fibres perfused with CsF inactivation of the Na channel is slow and incomplete (Adelman & Senft, 1966; Chandler & Meves, 1970*a*); the permeability of the Na channel for Cs ions is relatively small ($P_{\text{Na}}/P_{\text{Cs}} = 61$ or 58 for normal ionic strength (Chandler & Meves, 1965, 1970*a*)) and the delayed channel is almost completely blocked by internal Cs (Adelman & Senft, 1966; Chandler & Meves, 1965).

Action potentials from perfused fibres with 25 mM-CsF + glycerol as internal solution and 100 or 200 mM-CaCl₂ + glycerol as external solution have been described by Tasaki, Watanabe & Singer (1966) and Tasaki, Watanabe & Lerman (1967). The action potentials had an amplitude of 60-90 mV and lasted 0.1-20 sec at room temperature. They were blocked by tetrodotoxin (Watanabe, Tasaki, Singer & Lerman, 1967*b*), indicat-

ing, that at least part of the inward current is going through the Na channel.

We have done voltage clamp experiments to study the membrane currents underlying these action potentials. Our main objective was to measure the membrane potential at which the current through the Na channel reverses its sign. The reversal potential enabled us to estimate the relative permeability of the Na channel for Ca and Cs.

Further experiments were carried out to determine the relative permeability of the Na channel for Ca and Na. This was done by substituting NaF for the internal CsF or by adding NaCl to the external solution. We obtained permeability ratios P_{Ca}/P_{Na} between 1/10 and 1/7 which are considerably higher than the ratio 1/100 deduced from aequorin experiments on intact axons (Baker *et al.* 1971). A substantial loss of selectivity under our experimental conditions would be consistent with the observation that fibres with 5–50 mM-Na phosphate or NaF inside and 30–100 mM-CaCl₂ outside are still able to give action potentials (Watanabe, Tasaki & Lerman, 1967*a*).

Part of this work has already been described briefly (Meves & Vogel, 1972).

METHODS

Material

Giant axons with diameters between 600 and 1000 μm were obtained from large specimens of *Loligo forbesi* and occasionally *L. vulgaris*. Live squid were used sometimes but as a rule we employed mantles which had been stored for a few hours in ice-cold sea water.

Apparatus

The apparatus for voltage clamp was essentially the same as used previously (Chandler & Meves, 1965, 1970*a*). The internal electrode consisted of a 100 μm glass capillary for measuring the internal potential and a 70 μm platinum wire, for sending current, attached to the capillary; the distal 12 mm of the external platinum wire were carefully platinized. Membrane current density was determined by measuring the potential difference between two C-shaped Ag-AgCl electrodes positioned outside the fibre opposite the internal voltage electrode. The double C electrode was calibrated in the external solutions by sending a 10 μA current from a 12 mm platinized platinum wire, diameter 1 mm, centred in the double C.

Two modifications were introduced. (1) The feed-back amplifier was built from Philbrick operational amplifiers and was similar in design to that used by Bezanilla, Rojas & Taylor (1970). (2) A Grass P 18 differential amplifier was used to provide additional gain for the current record; the rise time of the amplifier was increased to 100 μsec in order to minimize noise.

Experimental procedure

The uncleaned axon was extruded and perfused with isotonic K₂SO₄ in the way described by Baker, Hodgkin & Shaw (1962). It was then tested and, if excitable,

was filled with 25 mM-CsF + sucrose or one of the other internal solutions given below. The fibre was washed for three consecutive periods of 8–10 min in Na-free Tris sea water and finally transferred to the experimental cell which contained 100 mM-CaCl₂ + sucrose or one of the other external solutions. The solution in the cell was kept at a temperature of 16–17° C.

TABLE 1. Composition of solutions

External solutions (concentrations in m-mole/l. solution)						
	Ca	Mg	Cl	Tris*	Sucrose	Acetate
Tris sea water	11	55	538	524	—	—
11 mM-CaCl ₂ + 55 mM-MgCl ₂ + sucrose†	11	55	132	—	689	—
10 mM-CaCl ₂ + 150 mM-Tris-HCl + sucrose	10	—	136	150	619	—
100 mM-CaCl ₂ + sucrose†	100	—	200	0.2	619	—
200 mM-CaCl ₂ + sucrose†	200	—	400	0.3	412	—
100 mM-Ca acetate + sucrose	100	—	—	—	619	200
Internal solutions						
	Concentrations m-mole/l. soln.		Activities§ m-mole/kg H ₂ O			
	Cs	Na	Cs	Na		
25 mM-CsF + sucrose‡	25	—	26	—		
22 mM-CsF + 3 mM-NaF + sucrose‡	22	3	22.75	3.25		
19 mM-CsF + 6 mM-NaF + sucrose‡	19	6	19.5	6.5		
Na phosphate with 15 mM-Na + sucrose	—	15	—	14		

* Total concentration of Tris = [Tris OH] + [Tris Cl].

† pH adjusted to 7.3–7.8 with 0.2–1.0 mM Tris-HCl buffer.

‡ pH adjusted to 7.3–7.5 with 0.2–1.0 mM Tris-HCl buffer.

§ From measurements with ion-selective electrodes (see text).

All resting potential measurements were corrected for junction potentials determined at the beginning and end of each experiment (see Baker, Hodgkin & Meves, 1964).

In several experiments a hyperpolarizing holding current was used; the membrane was held at the holding potential for a period of 3 min before taking the voltage clamp records.

In the first experiments the fibres were internally treated with pronase in order to remove remnants of axoplasm, a technique routinely employed by Tasaki and coworkers. We used a solution of 25 mM-CsF + sucrose with 0.05 mg pronase/ml., applied internally for 90 sec at the start of the experiment. The majority of the experiments were done without pronase treatment.

Solutions

The composition of the external and internal solutions is given in Table 1. Sucrose was used to maintain isotonicity. 1 molal sucrose (1.0 mole/kg H₂O = 825 m-mole/l. solution) and 0.4 M-CaCl₂ were considered as isotonic with sea water. 111 mM-Tris-

HCl were assumed to be osmotically equivalent to 100 mM-NaCl. Diluted solutions of CsF, NaF or Na phosphate were used for internal perfusion. They were obtained by mixing isotonic solutions of these salts (0.6 M-CsF; 0.6 M-NaF; 0.35 M-Na phosphate at pH 7.2) with isotonic sucrose. The Na activities given in Table 1 were determined at 16–18° C with a Na-sensitive glass electrode. The Cs activity in 25 mM-CsF + sucrose was assumed to be the same as the K activity in 25 mM-KF + sucrose; the latter was measured with a K-sensitive electrode.

The pH was 7.3–7.8 for the external solutions and 7.3–7.5 for the internal solutions and was adjusted with Tris-HCl buffer (final concentration 0.2–1.0 mM). In the experiment of Fig. 6 the internal 25 mM-CsF + sucrose solution contained additional 5 mM-Tris-HF buffer of pH 7.2.

TABLE 2. Ca and Na activities in the external solutions

Solution	(2)		(3)	(4)	(5)	(6)
	Ca concentration		γ_{CaCl_2}	Ca activity m-mole kg H ₂ O	Na con- centra- tion m-mole l. soln.	Na activity m-mole kg H ₂ O
	m-mole	m-mole				
	l. soln	kg H ₂ O				
Calibration solutions for Ca electrode	—	14.4	0.70	7.0	—	—
	—	78.4	0.54	23.1	—	—
	—	100	0.52	27.4	—	—
	—	200	0.48	45.6	—	—
	—	300	0.46	63.6	—	—
10 mM-CaCl ₂ + 150 mM-Tris- HCl + sucrose	10	—	—	5 (6.5)	—	—
100 mM-CaCl ₂ + sucrose	100	115.5	—	35.5 (71)	—	—
200 mM-CaCl ₂ + sucrose	200	220.5	—	51 (109)	—	—
100 mM-Ca acetate + sucrose	100	—	—	32.0	—	—
100 mM-CaCl ₂ + 5 mM-NaCl + sucrose	99	—	—	35.5	5	6
100 mM-CaCl ₂ + 25 mM-NaCl + sucrose	95.5	—	—	33	25	26.5
100 mM-CaCl ₂ + 50 mM NaCl + sucrose	91.5	—	—	31.5	50	51

Column (3): γ_{CaCl_2} from Robinson & Stokes (1959) for 15° C. Column (4): Ca activities in the calibration solutions calculated for $\gamma_{\text{Ca}^{2+}} = (\gamma_{\text{CaCl}_2})^2$, Ca activities in the experimental solutions from measurements with a Ca-selective electrode. Column (6): Na activities from measurements with a Na-selective electrode, using NaCl solutions of concentration 1.6–57.9 m-mole/kg H₂O as calibration solutions and data for γ_{NaCl} (= γ_{Na^+}) from Robinson & Stokes.

Measurements of the Ca activity in the external solutions were made at room temperature with a Beckman Ca electrode calibrated in solutions of known activity coefficient γ_{CaCl_2} . For the single ion activity coefficient $\gamma_{\text{Ca}^{2+}}$ several conventions exist (Shatkay, 1968; Bates & Alfenaar, 1969). We used the convention $\gamma_{\text{Ca}^{2+}} = (\gamma_{\text{CaCl}_2})^2$ to calculate the Ca²⁺ activity in the calibration solutions. The Ca²⁺ activities in the calibration solutions (calculated from $\gamma_{\text{Ca}^{2+}} = (\gamma_{\text{CaCl}_2})^2$) and in the experimental solutions (measured with the Ca electrode) are given in column 4

of Table 2. The drift of the Ca electrode was larger in the experimental solutions than in the calibration solutions, probably due to the high concentrations of sucrose in the experimental solutions. The values in column 4 are averages from several measurements made after equilibrating the electrode for 2 min in the respective solution. For three of the main experimental solutions the Ca^{2+} activities obtained under the convention $\gamma_{\text{Ca}^{2+}} = \gamma_{\text{CaCl}_2}$ are added in brackets.

External solutions with small concentrations of NaCl were obtained by adding small amounts of 0.6 M-NaCl to the Na-free solution in the experimental cell. The dilution led to a slight decrease of the Ca concentration. The resulting solutions are given in the last three lines of Table 2. The Na activity in these solutions was determined with a Na-selective electrode (column 6 of Table 2).

The Na contaminations of the Tris sea water and the 100 mM- CaCl_2 + sucrose solution were measured with an EEL flame photometer (Evans Electroelenium Ltd) and were found to be 0.07 and 0.38 mM respectively.

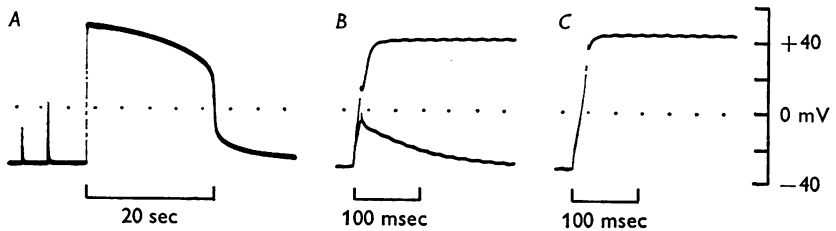


Fig. 1. Action potentials elicited by current pulses applied through the internal wire. External solution: 100 mM- CaCl_2 + sucrose. Internal solution: 25 mM-CsF + sucrose. *A*: slow time base, three 20 msec current pulses of increasing strength, third pulse suprathreshold. *B*: fast time base, two 10 msec current pulses, one just suprathreshold. *C*: fast time base, 20 msec current pulse. Resting potential -32.5 mV. Records were taken 100 min after removal of Na from the external solution. Axon 4, diameter $665 \mu\text{m}$. Temperature 16°C .

RESULTS

Resting and action potential

With 100 mM- CaCl_2 + sucrose outside and 25 mM-CsF + sucrose inside the resting potential was between -20 and -40 mV. Fig. 1 shows typical action potentials on two different time bases. Short current pulses of varying strength, applied through the internal current wire, were used for stimulation. The threshold potential was estimated as 0 mV. The overshoot was 46–48 mV in *A* and *C* and 42 mV in *B*. The action potential lasted 20 sec and was followed by a slowly decaying after-depolarization.

An important feature of these action potentials is their slow rising phase. This is best seen with a just suprathreshold stimulus as in Fig. 1*B*. The short stimulating pulse lowered the internal potential to $+11.5$ mV. From there the inward current depolarized the membrane by further 22 mV within 11 msec. This fairly rapid phase was followed by a slower depolarization which brought the potential to the peak of the action

potential. During the rapid phase the rate of rise was 2 V/sec, i.e. much smaller than the maximum rate of 400 V/sec for a normal action potential. A rate of rise of 2 V/sec corresponds to an inward current of $1.8 \mu\text{A}/\text{cm}^2$ if the membrane capacity is taken as $0.9 \mu\text{F}/\text{cm}^2$.

Action potentials similar to those in Fig. 1 were recorded in another seven fibres. The overshoot was 40–60 mV. The duration of the action potentials varied considerably and ranged between 5 and 40 sec for fresh fibres at 16–17° C. All of them showed a slow after-depolarization. In one of these experiments the rising phase was recorded on a fast time base as in Fig. 1B; its steepest part lasted again 11 msec and had a slope of 1.7 V/sec.

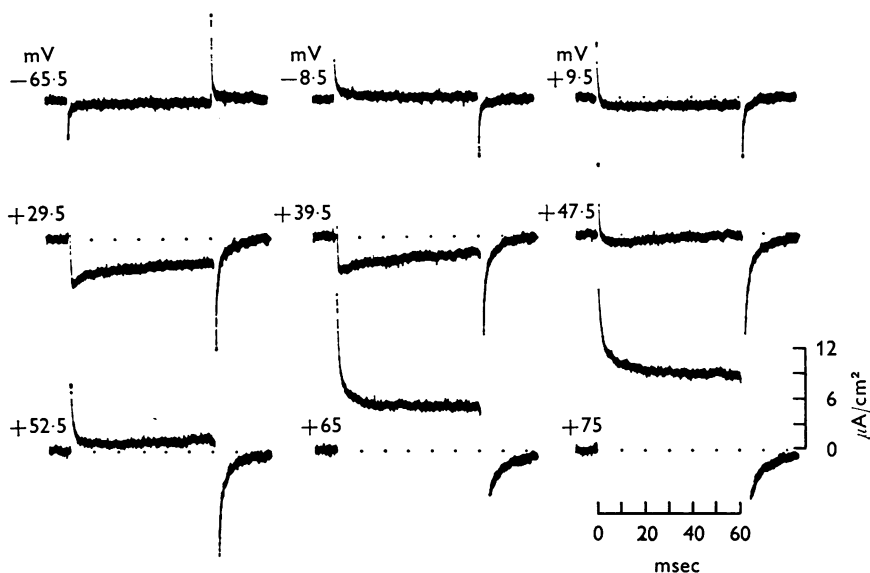


Fig. 2. Membrane currents associated with step changes in membrane potential. External solution: 100 mM-CaCl₂ + sucrose. Internal solution: 25 mM-CsF + sucrose. Resting potential = holding potential = -37.5 mV. The internal potential during the potential step is given above each trace. Outward current upward. The current tails at the end of the two largest pulses (+65 and +75 mV) were partly off screen. Records were taken 72 min after the removal of Na from the external solution. The leakage resistance, estimated from hyperpolarizing pulses, was $80 \text{ k}\Omega \text{ cm}^2$. Axon 41, diameter $840 \mu\text{m}$. Temperature 16.9°C .

Membrane currents in 100 mM-CaCl₂ + sucrose

From the shape and duration of the action potential it can be predicted that the net inward current during a depolarizing clamp pulse will be of the order of a few $\mu\text{A}/\text{cm}^2$ and will inactivate very slowly. The voltage clamp records in Fig. 2 confirm this prediction. A clamp pulse to

+9.5 mV produced a small inward current. The current reached a maximum of -5 to $-6 \mu\text{A}/\text{cm}^2$ at a potential of +29.5 mV and became smaller for larger depolarizations. At +52.5 mV the current was outward during the whole pulse. With stronger pulses the outward current grew rapidly in size. The inward and outward currents were maintained during the whole 60 msec clamp pulses. There was, however, a clear decay of the inward currents and a lesser decay of the outward currents as best seen in the records labelled +29.5, +39.5 and +75 mV. Hyperpolarizing pulses like the pulse to -65.5 mV were used to estimate the leakage resistance; it was obtained as $80 \text{ k}\Omega \text{ cm}^2$.

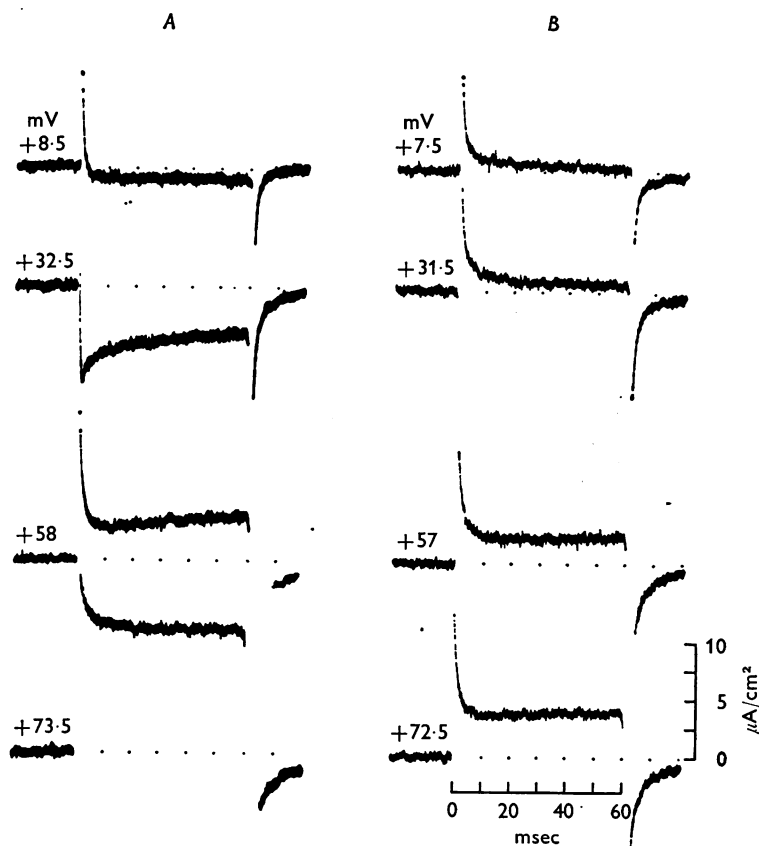


Fig. 3. Effect of tetrodotoxin on membrane currents. *A*: 100 mM- CaCl_2 + sucrose (without tetrodotoxin) as external solution. *B*: 18 min after adding tetrodotoxin, final concentration $2 \mu\text{M}$. Internal solution: 25 mM- CsF + sucrose. *A*, resting potential = holding potential = -44.5 mV; *B*, resting potential = -35.5 mV, holding potential = -45.5 mV. Records in *A* were taken 65 min after removal of Na from the external solution. Axon 42, diameter $960 \mu\text{m}$. Temperature 17.0°C .

The next step was to find out whether the membrane currents were affected by tetrodotoxin, the selective inhibitor of the sodium channel. As illustrated in Fig. 3, the inward currents were completely abolished by $2 \mu\text{M}$ tetrodotoxin. The drug also considerably reduced the size of the outward currents.

Closer inspection of the records in Fig. 3*B* shows that the capacity transients seem to last for 10–20 msec. This is much longer than expected from the size of the series resistance and the membrane capacitance. The series resistance was estimated as $55 \Omega \text{ cm}^2$ from measurements of the resistivity of the external and internal solution (96 and $365 \Omega \text{ cm}$, respectively). Hence, for a membrane capacitance of $0.9 \mu\text{F}/\text{cm}^2$ the time constant of the capacity transient would be $50 \mu\text{sec}$. The slow transients in the two uppermost records of Fig. 3*B*, however, decay with a time constant of 4.4–5.6 msec. The slow component of the capacity transient is best seen in tetrodotoxin-treated fibres (Figs. 3*B*, 9*D* and 11*C*). A similar slow tail of the capacity transient has been described by other authors (e.g. Hodgkin, Huxley & Katz, 1952; Moore, Narahashi, Poston & Arispé, 1970) and has been attributed to the imperfection of the membrane capacitance.

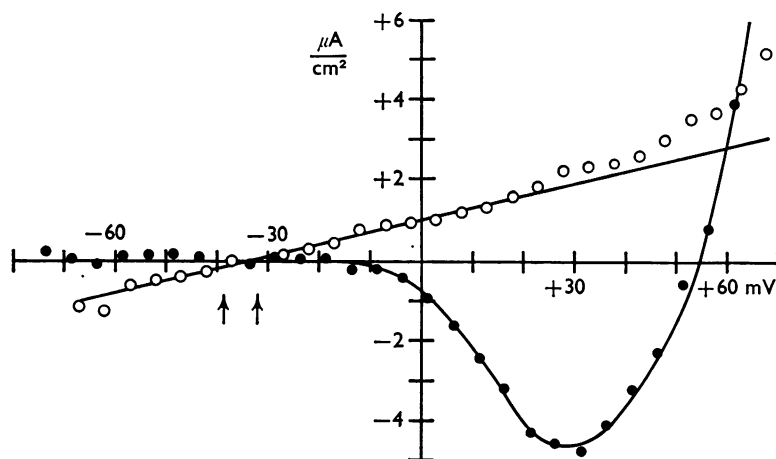


Fig. 4. Current-voltage relation for a fibre with 100 mM-CaCl_2 + sucrose outside and 25 mM-CsF + sucrose inside. The membrane current is split into its two components, the tetrodotoxin-sensitive and the tetrodotoxin-insensitive current. ●, tetrodotoxin-sensitive current = (current before application of tetrodotoxin) – (current after application of tetrodotoxin), ○, tetrodotoxin-insensitive current = current after application of tetrodotoxin. The currents before application of tetrodotoxin were recorded with a holding potential of -38.5 mV (= resting potential). The currents after application of tetrodotoxin were recorded 16 min after adding tetrodotoxin (final concentration $1.5 \mu\text{M}$), resting potential = holding potential = -32 mV . Holding potentials indicated by arrows. All currents were measured 20 msec after beginning of clamp pulse. Abscissa: internal potential during pulse. A straight line with a slope of $33.1 \text{ k}\Omega \text{ cm}^2$ was drawn through the linear portion of the tetrodotoxin-insensitive current. Axon 15, diameter $990 \mu\text{m}$. Temperature 16.5°C .

The quantitative analysis of a tetrodotoxin experiment is presented in Fig. 4. The open circles (○) give the membrane currents recorded in the presence of $1.5 \mu\text{M}$ tetrodotoxin and measured 20 msec after the beginning of the clamp pulse. The time 20 msec (or 10 msec in other experiments) was chosen because it is outside the duration of the long lasting capacity transient. The measuring points follow a straight line, drawn with a slope of $33.1 \text{ k}\Omega \text{ cm}^2$, over a wide potential range, but deviate clearly for internal potentials larger than 25 mV. The same deviation was seen if the currents were measured 60 msec after the beginning of the clamp pulse. A deviation of this kind was found in all experiments, but to varying degrees. It was also observed in a chloride-free external medium (Fig. 6) and in experiments with 50 mM tetraethylammonium chloride added to the internal solution. It seems that the current responsible for the deviation is carried by internal Cs ions going through the leakage channel ('leakage rectification'; see Adelman & Taylor, 1961).

The filled circles (●) in Fig. 4 represent the tetrodotoxin-sensitive current, i.e. (current before application of tetrodotoxin) - (current after application of tetrodotoxin). The currents are again measured 20 msec after the beginning of the clamp pulse which is approximately the time at which the net inward current reaches its peak. As mentioned in the legend of Fig. 4, the resting potential dropped by 6.5 mV during the experiment. The change in resting potential was taken into account by assuming that the non-linear portion of the tetrodotoxin-insensitive current is determined by the absolute potential whereas the linear portion is proportional to the potential change.

As illustrated by Fig. 4, the tetrodotoxin-sensitive current was inward for small depolarizations, reversed its sign between +50 and +60 mV internal potential and became outward for larger depolarizations. The inward current started to turn on between -10 and 0 mV and reached its peak ($4.5 \mu\text{A}/\text{cm}^2$) around +25 to +30 mV. These findings are in agreement with Figs. 2 and 3.

The reversal potential (or equilibrium potential) of the tetrodotoxin-sensitive current was $V_e = +54.5 \text{ mV}$ in Fig. 4. Further values for V_e from a total of ten fibres with an average of $V_e = +54.1 \text{ mV}$ are given in Table 3A.

Approximate values for the reversal potential of the tetrodotoxin-sensitive current were obtained by correcting the current records around V_e for a linear leakage current, i.e. by subtracting the current produced by a hyperpolarizing pulse and scaled to the proper voltage. This method neglects the rectification in the tetrodotoxin-insensitive current. The resulting error in V_e is, however, small. Using this approximate method for the experiment of Fig. 4 a reversal potential of +51.5 mV (instead of

+54.5 mV) was obtained. The reversal potentials of ten fibres as determined by the approximate method are listed in Table 3*B*.

The last columns in Table 3*A* and *B* give the time spent in Na-free solution before taking the voltage clamp records. Plotting the reversal potential V_e against time in Na-free solution appeared to indicate a slight tendency of V_e to decrease with increasing time. Closer analysis gave a correlation coefficient of 0.44 which is not significant for nineteen pairs of observations, even on the $P = 0.05$ level. This negative result is important because it makes it unlikely that the measurements of V_e are falsified by incomplete removal of Na ions from the extracellular space.

TABLE 3. Reversal potential V_e of tetrodotoxin-sensitive current in fibres with 100 mM-CaCl₂ + sucrose outside and 25 mM-CsF + sucrose inside

(A) From records without and with tetrodotoxin				(B) From leakage correction			
Axon	V_e (mV)	Temp. (°C)	Time in Na-free soln. (min)	Axon	V_e (mV)	Temp. (°C)	Time in Na-free soln. (min)
10†	51.5	15.8	88	9†	52	15.7	105
12†	55.5	16.1	73	13	39.5	16.7	80
15	54.5	16.5	107	14	50.5	16.2	203
16	50	16.7	101	17	54	16.5	147
19	57	16.2	60	18	48.5	16.5	118
21	61	16.4	60	20	49.5	16.5	59
30	37.5	15.8	156	32	54	16.0	97
34	60.5	16.0	55	39	54	16.2	99
41	57.5	16.9	72	40	55	16.2	133
42	55.5	17.0	65	Average	50.8	—	—
Average	54.1	—	—	s.e.	± 1.6	—	—
s.e.	± 2.1	—	—	33	41	-0.6	65

* Clamp run in 100 mM-CaCl₂ + sucrose directly followed by run in 100 mM-CaCl₂ + sucrose + 1.5 or 2 μM-tetrodotoxin, except for axons 19, 21 and 34 where clamp runs with 5–10 mM-Na added to the internal or external solution were interposed.

† Pre-treated with pronase for 90 sec (see Methods).

The time course of the tetrodotoxin-sensitive current is shown in Fig. 5. As in Fig. 4 the tetrodotoxin-sensitive current was inward for internal potentials between +1.5 and +51.5 mV, but outward for a potential of +61.5 mV. The curves for +16.5 to +51.5 mV reveal a fairly fast decay of the tetrodotoxin-sensitive inward current during the first 20–30 msec; it followed an exponential time course with a time constant of 10–20 msec. After this initial decay the tetrodotoxin-sensitive inward current declined

more slowly. Experiments with longer pulses indicated that even after 300 msec there was still a large fraction of the inward current left.

The tetrodotoxin-sensitive outward current stayed constant during a 60 msec pulse as shown by record +61.5 mV in Fig. 5 (see also records +73.5 and +72.5 mV in Fig. 3*A* and *B*). However, a slow decay of the outward current was seen in Fig. 2 (60 msec pulse to +75 mV) and with longer pulses.

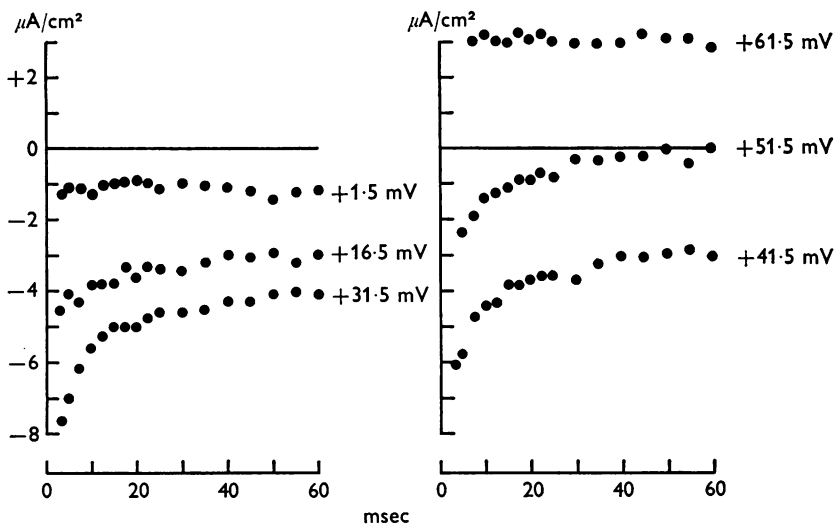


Fig. 5. Time course of the tetrodotoxin-sensitive current for a fibre with 100 mM-CaCl₂ + sucrose outside and 25 mM-CsF + sucrose inside. Same experiment as in Fig. 4. Ordinate: tetrodotoxin-sensitive current = (current before application of tetrodotoxin) - (current after application of tetrodotoxin). Abscissa: time after beginning of clamp pulse. The internal potential during the clamp pulse is given beside each curve.

Membrane currents in 100 mM-Ca acetate and 100 mM-MgCl₂ + sucrose

The aim of these experiments was to demonstrate that under our experimental conditions the inward currents are carried by external Ca²⁺ (and not by internal F⁻ or residual external Na⁺) and the outward currents by internal Cs⁺ (and not by external Cl⁻). Fig. 6 shows an experiment in which the external Cl⁻ was replaced by acetate, an anion which does not seem to permeate through the membrane of frog and barnacle muscle fibres (Falk & Landa, 1960; Hagiwara, Chichibu & Naka, 1964). The experiment was otherwise identical with that in Fig. 4. The tetrodotoxin-sensitive and the tetrodotoxin-insensitive current are again represented by ● and ○. The main point of interest is that the tetrodotoxin-sensitive outward current is still present. We therefore conclude that it is not

carried by external Cl^- ; it is probably carried by Cs^+ ions moving outwards through the Na channel.

The reversal potential of the tetrodotoxin-sensitive current in Fig. 6 is +43 mV. This is somewhat smaller than the reversal potentials in 100 mM- CaCl_2 + sucrose (Table 3); part of this difference may be due to the slightly smaller calcium activity in the 100 mM-Ca acetate + sucrose solution (Table 2). The non-linearity of the tetrodotoxin-insensitive current is preserved (see p. 234). The only major difference between Fig. 6 and Fig. 4 is the smaller size and larger scattering of the tetrodotoxin-sensitive current in the Ca acetate experiment, indicating that acetate is not an ideal substitute for Cl^- .

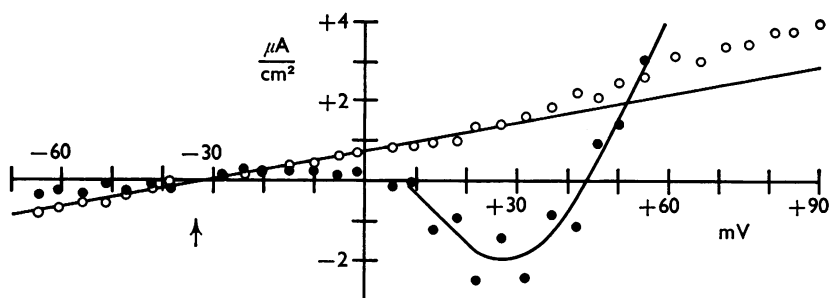


Fig. 6. Current-voltage relation for a fibre with 100 mM-Ca acetate + sucrose outside and 25 mM-CsF + 5 mM-Tris-HF + sucrose inside. ●, tetrodotoxin-sensitive current = (current before application of tetrodotoxin) - (current after application of tetrodotoxin). ○, tetrodotoxin-insensitive current = current after application of tetrodotoxin. The currents before application of tetrodotoxin were recorded with a holding potential of -33.5 mV (= resting potential). The currents after application of tetrodotoxin were recorded 22 min after adding tetrodotoxin (final concentration 1.5 μM), resting potential = -18.5 mV, holding potential = -33.5 mV. Holding potential indicated by arrow. All currents were measured 20 msec after beginning of clamp pulse. Abscissa: internal potential during pulse. A straight line with a slope of 41.8 $\text{k}\Omega \text{ cm}^2$ was drawn through the linear portion of the tetrodotoxin-insensitive current. Axon 31, diameter 860 μm . Temperature 15.9° C.

A possible explanation for the unfavourable effect of acetate is that undissociated molecules of acetic acid move from the external to the internal solution, lower the internal pH and thereby reduce the size of the tetrodotoxin-sensitive current (Chandler & Meves, 1965; Ehrenstein & Fishman, 1971). The additional 5 mM-Tris-HF buffer which the internal solution contained for this experiment (see legend Fig. 6) was probably not sufficient to prevent a drop of the internal pH.

Inward currents were not observed when the external Ca was replaced by Mg. Fig. 7A shows membrane currents from an experiment with 100 mM- MgCl_2 + sucrose as external solution. The current-voltage curve was

perfectly linear for internal potentials between -90 and $+25$ mV and had a slope of 29.7 k Ω cm 2 . At more positive potentials the outward current increased markedly (see record 48.5 mV). The absence of inward currents in Fig. 7A cannot be attributed to inexcitability because large inward currents were observed after adding 20 mM-NaCl to the external

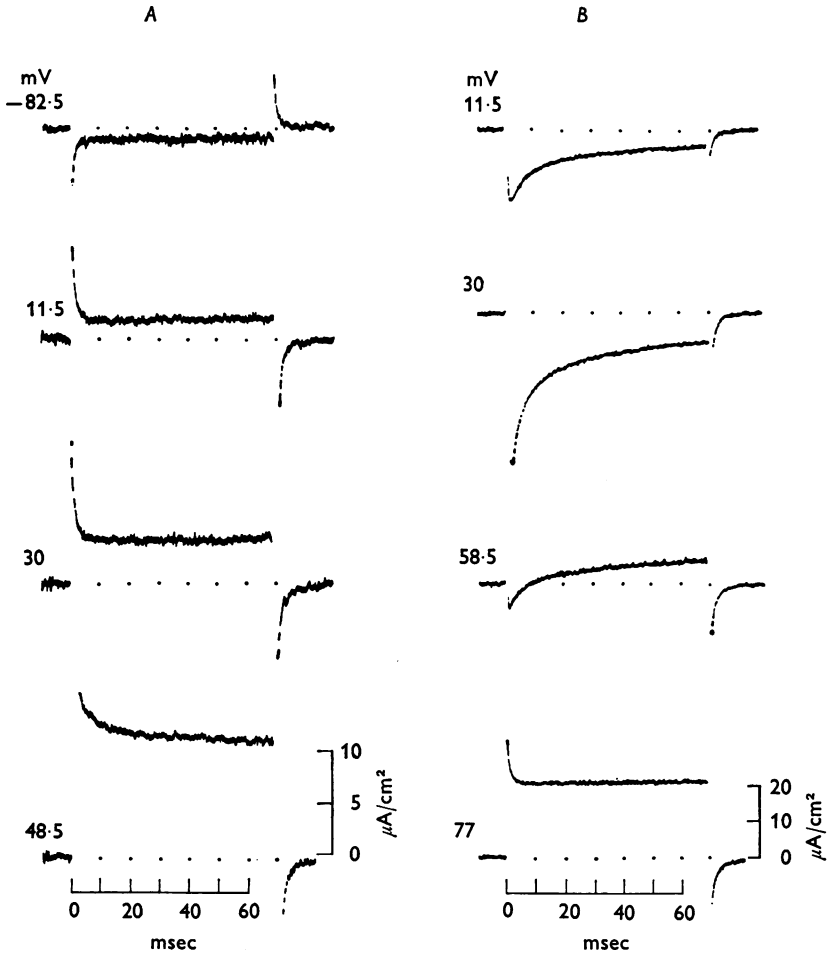


Fig. 7. Membrane currents in the absence of external Ca. External solution: A, 100 mM-MgCl $_2$ + sucrose; B, 100 mM-MgCl $_2$ + 20 mM-NaCl + sucrose. Internal solution: 25 mM-CsF + sucrose. Records in A were taken 55 min after the removal of Na from the external solution, resting potential -24.5 mV, holding potential -54.5 mV. Records in B were taken 14 min after adding NaCl (final concentration 20 mM), resting potential -14.5 mV, holding potential -54.5 mV. Note lower gain in B. Axon 36, diameter 915 μm . Temperature 16.4°C .

solution (Fig. 7*B*). (The effect of external Na is fully discussed on pp. 247–252.)

Another experiment with 100 mM-MgCl₂ + sucrose as external solution is shown in Fig. 8*A*. Again, no net inward currents were found. Records labelled 16 and 34.5 mV reveal, however, an apparent time dependence of the outward current which could be due to a small transient inward current; this was not further analysed. Fig. 8*B* demonstrates that the same fibre gave large net inward currents with 100 mM-CaCl₂ + sucrose outside.

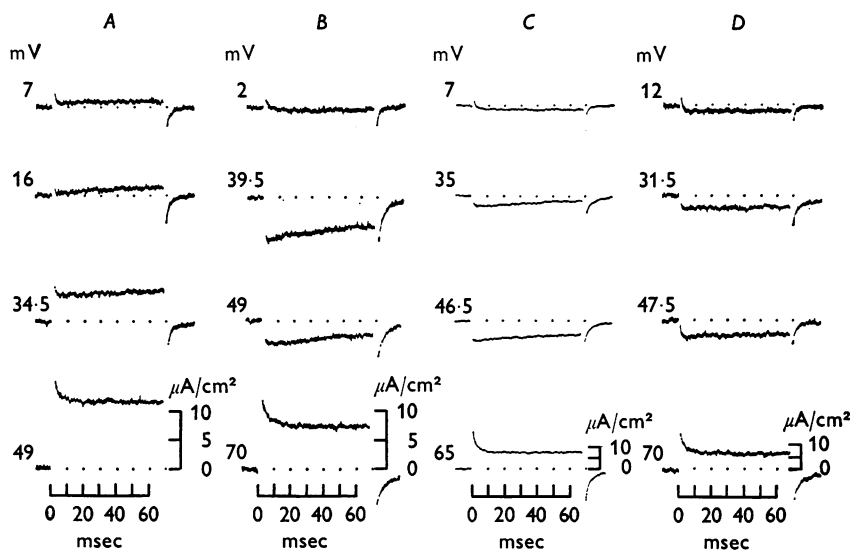


Fig. 8. Membrane currents from a fibre perfused with 25 mM-CsF + sucrose and in various external solutions. *A*, 100 mM-MgCl₂ + sucrose, resting potential -21 mV, holding potential -41 mV; *B*, 100 mM-CaCl₂ + sucrose, resting potential -46 mV, holding potential -36 mV; *C*, 100 mM-CaCl₂ + sucrose, resting potential = holding potential = -50 mV; *D*, 200 mM-CaCl₂ + sucrose, resting potential = holding potential = -53.5 mV. Records were taken in the sequence *A*, *C*, *B*, *D*. *C* and *D* at lower current gain than *A* and *B*. Axon 32, diameter 850 μm. Temperature 16.0° C.

The records in column *B* were taken at a less negative holding potential than those in *A* in order to compensate for the different position of the inactivation curve in 100 mM-MgCl₂ and in 100 mM-CaCl₂. Larger inward currents were obtained with a more negative holding potential in Fig. 8*C*. (The records in Fig. 8*C*-*D* are discussed in the following chapter.)

The experiments in Figs. 7 and 8 can be summarized by saying that the fibres gave no net inward currents in 100 mM-MgCl₂ + sucrose, although they were fully excitable in this solution after adding a small amount of Na. This makes it unlikely that the inward currents seen with 100 mM-

CaCl_2 + sucrose are carried by internal F^- or residual external Na^+ . We conclude therefore that the tetrodotoxin-sensitive inward current is carried by Ca ions moving through the Na channel. At the reversal potential of the tetrodotoxin-sensitive current the Ca current is equal and opposite to the Cs current. Further experiments were done to study the effect of altering the external Ca concentration on the reversal potential.

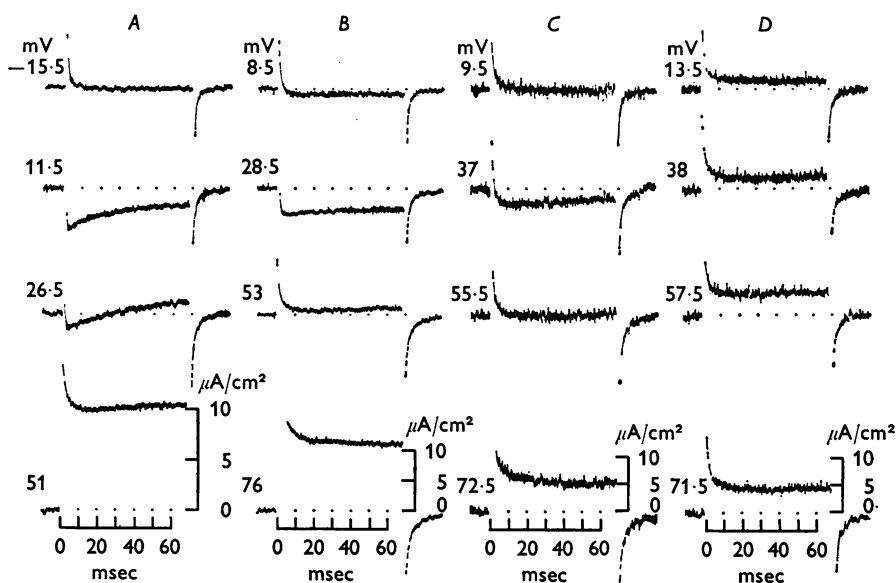


Fig. 9. Effect of external Ca concentration on membrane currents. *A*, 10 mM- CaCl_2 + 150 mM-Tris-HCl + sucrose, resting potential -19 mV, holding potential -49 mV. *B*, 100 mM- CaCl_2 + sucrose, resting potential -27 mV, holding potential -47 mV. *C*, 200 mM- CaCl_2 + sucrose, resting potential -39.5 mV, holding potential -59.5 mV. *D*, 200 mM- CaCl_2 + sucrose + $1.5 \mu\text{M}$ -tetrodotoxin, resting potential -45.5 mV, holding potential -65.5 mV. Records in *D* were taken 19 min after adding tetrodotoxin. Internal solution: 25 mM-CsF + sucrose. Note different current gains. Axon 40, diameter $780 \mu\text{m}$. Temperature 16.2°C .

Effect of external Ca concentration on membrane currents

Fig. 8*C* and *D* show that the inward currents in 100 and 200 mM- CaCl_2 + sucrose have about the same size and time course. (The records in *D* show more noise than those in *C* because the gain was increased to compensate for the lower recording resistance in 200 mM- CaCl_2 + sucrose.) This finding is supported by the more complete experiment in Figs. 9 and 10. It consists of voltage clamp runs in 10, 100 and 200 mM- CaCl_2 + sucrose and is concluded with voltage clamp records in 200 mM- CaCl_2 + sucrose +

1.5 μM tetrodotoxin. The latter are needed for an accurate determination of the reversal potential of the tetrodotoxin-sensitive current.

The first point to be discussed is the effect of external Ca on the resting potential. As can be seen from the values given in the legend of Fig. 9, the absolute value of the resting potential increased with increasing $[\text{Ca}]_o$. The hyperpolarization following the change from 100 to 200 mM-CaCl₂ was 12.5 mV in the experiment of Figs. 9 and 10, 3.5 mV in the experiment

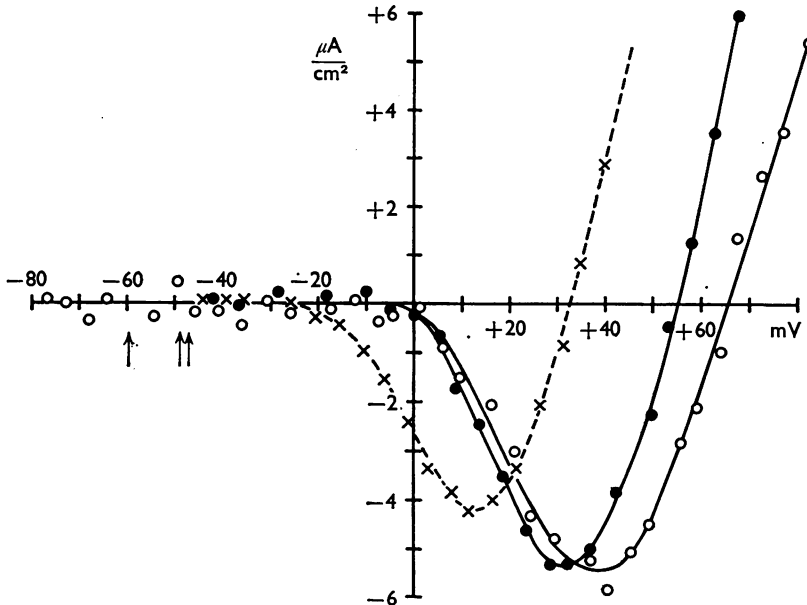


Fig. 10. Effect of external Ca concentration on current-voltage relation. Same experiment as in Fig. 9. \times , Current in 10 mM-CaCl₂ + 150 mM-Tris-HCl + sucrose (Fig. 9A), corrected for leakage current. \bullet ; current in 100 mM-CaCl₂ + sucrose (Fig. 9B), corrected for leakage current; \circ , tetrodotoxin-sensitive current in 200 mM-CaCl₂ + sucrose = current before application of tetrodotoxin (Fig. 9C) - current after application of tetrodotoxin (Fig. 9D). Holding potentials indicated by arrows. All currents were measured 10 msec after beginning of clamp pulse. Abscissa: internal potential during pulse.

of Fig. 8 and 11 mV in a third experiment. Contrary to our observations Tasaki *et al.* (1967) have found a depolarization for increasing $[\text{Ca}]_o$. Possible reasons for this discrepancy are discussed on p. 261.

Another unexpected finding was the relatively large size of the inward current in 10 mM-CaCl₂ (Fig. 9A, \times in Fig. 10). The maximum inward current in 10 mM-CaCl₂ amounted to 81% of the maximum current in 100 mM-CaCl₂ (\bullet in Fig. 10) although the Ca activity in the external

solution was seven times smaller (see Table 2). The inward current in 200 mM-CaCl₂ (○ in Fig. 10) was about the same as that in 100 mM-CaCl₂ although the Ca activity was 1.4 times larger. A possible explanation is that the maximum permeability of the Na channel which is reached at large depolarizations decreases with increasing external Ca concentration. This explanation is supported by observations of Blaustein & Goldman (1968) and Hille (1968) who found a decrease of the maximum Na conductance in high concentrations of Ca or other polyvalent cations.

In Fig. 10 the negative resistance branch of the current-voltage curve is shifted towards more positive internal potentials as the external Ca concentration increases. This effect is probably due to a shift of the relation between permeability and voltage; the voltage dependence of the permeability coefficient as calculated from the currents in Fig. 10 by means of the constant field equations (eqns (2) and (4) on p. 253 with $V' = +50$ mV) showed a similar shift. The shift of the negative resistance branch of the current-voltage curve was 15–17 mV for the change from 10 to 100 mM and 3–4 mV for the change from 100 to 200 mM. These findings are roughly consistent with the 15 mV shift per fivefold change in Ca concentration reported by Frankenhaeuser & Hodgkin (1957).

The main objective of the experiment in Figs. 9 and 10 was to study the effect of external Ca on the reversal potential V_e of the tetrodotoxin-sensitive current. V_e in 200 mM-CaCl₂ was found by plotting the tetrodotoxin-sensitive current (= current before application of tetrodotoxin – current after application of tetrodotoxin) against the internal potential (○ in Fig. 10). This gave $V_e = +65.5$ mV. The approximate method for determining V_e which consists in subtracting a linear leakage (see p. 234) led to the somewhat smaller value of +60.5 mV. For 100 and 10 mM-CaCl₂ only the approximate method could be used. The corrected current-voltage curve for 100 mM-CaCl₂ (● in Fig. 10) gave $V_e = +55$ mV which agrees well with the average values in Table 3*A* and *B*. For 10 mM-CaCl₂ (× in Fig. 10) the reversal potential was obtained as $V_e = +32.5$ mV.

A second experiment gave $V_e = +68$ mV in 200 mM-CaCl₂ (from subtraction of tetrodotoxin-insensitive current), $V_e = +54$ mV in 100 mM-CaCl₂ (from subtraction of linear leakage current) and $V_e = +32$ mV in 10 mM-CaCl₂ (from subtraction of linear leakage current). Two further experiments with voltage clamp runs in 10 mM-CaCl₂ without and with 1.5 μM tetrodotoxin gave the reversal potential of the tetrodotoxin-sensitive current in 10 mM-CaCl₂ as +30 and +36.5 mV which is in good agreement with the values obtained by subtracting a linear leakage current.

Net inward currents were also seen with 11 mM-CaCl₂ + 55 mM-MgCl₂ + sucrose as external solution, but not in Tris sea water with 11 mM-CaCl₂

and 55 mM-MgCl₂. The negative result with Tris sea water is probably due to the fact that the leakage resistance in Tris sea water is two or three times smaller than in 11 mM-CaCl₂ + 55 mM-MgCl₂ + sucrose; subtraction of the leakage current revealed small inward currents in Tris sea water.

Effect of internal Na on membrane currents

The experiments so far described were done with 25 mM-CsF + sucrose inside and varying CaCl₂ concentrations outside. They allow a quantitative estimate of the permeability ratio P_{Ca}/P_{Cs} (see below). To obtain information about the ratio P_{Ca}/P_{Na} further experiments with Na in the internal or external solution were done.

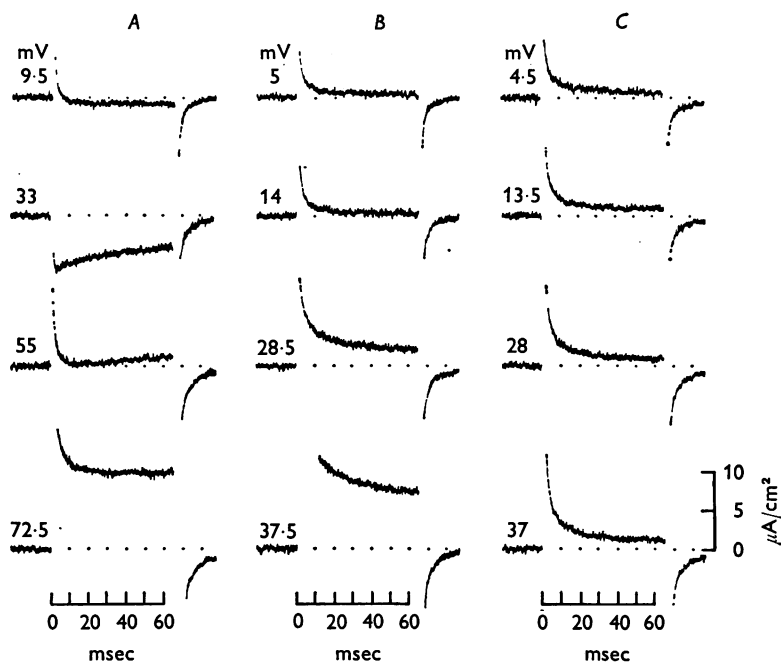


Fig. 11. Effect of internal Na on membrane currents. *A*, 25 mM-CsF + sucrose inside, 100 mM-CaCl₂ + sucrose outside, resting potential = holding potential = -42.5 mV. *B*, 6 mM-NaF + 19 mM-CsF + sucrose inside, 100 mM-CaCl₂ + sucrose outside, resting potential = holding potential = -38 mV. *C*, 6 mM-NaF + 19 mM-CsF + sucrose inside, 100 mM-CaCl₂ + sucrose + 1.5 μM-tetrodotoxin outside, resting potential -28.5 mV, holding potential -38.5 mV. Records in *C* were taken 20 min after adding tetrodotoxin. Axon 34, diameter 990 μm. Temperature 16.0° C.

Figs. 11 and 12 illustrate an experiment in which the internal solution was changed from 25 mM-CsF + sucrose to 6 mM-NaF + 19 mM-CsF + sucrose. With 25 mM-CsF inside (column *A* in Fig. 11) the currents

followed their usual pattern: a maximum inward current near +30 mV, a change of sign around +50 or +60 mV, a strong outward current at more positive potentials. Replacing a quarter of the internal CsF by NaF led to the complete disappearance of the net inward current (column *B* in Fig. 11). Subtraction of the tetrodotoxin-insensitive current (column *C* in Fig. 11), however, revealed that there was still a small tetrodotoxin-sensitive inward current present (compare records 14 mV in Fig. 11*B* and 13.5 mV in Fig. 11*C*).

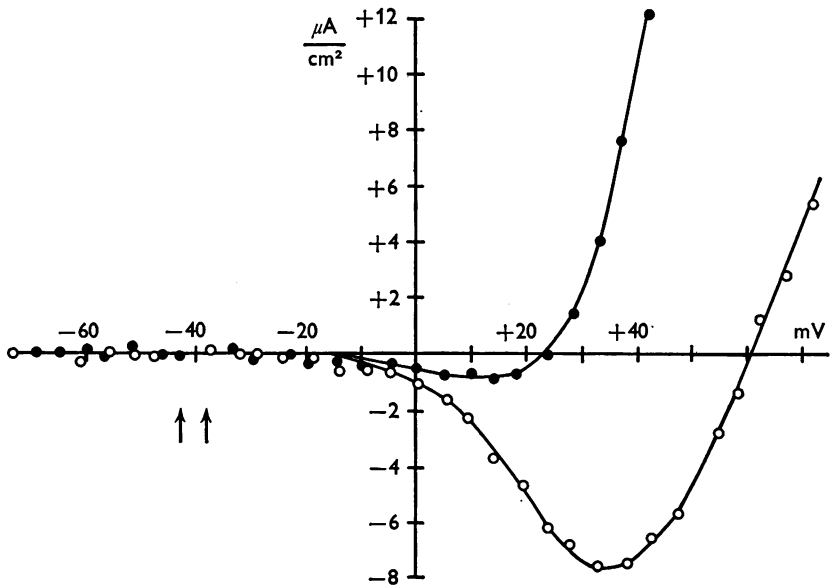


Fig. 12. Effect of internal Na on current-voltage relation. Same experiment as in Fig. 11. ○, Tetrodotoxin-sensitive current with 25 mM-CsF + sucrose inside = current with 25 mM-CsF + sucrose inside before application of tetrodotoxin (Fig. 11*A*) – current after application of tetrodotoxin (Fig. 11*C*); ●, tetrodotoxin-sensitive current with 6 mM-NaF + 19 mM-CsF + sucrose inside = current with 6 mM-NaF + 19 mM-CsF + sucrose inside before application of tetrodotoxin (Fig. 11*B*) – current after application of tetrodotoxin (Fig. 11*C*). Holding potentials indicated by arrows. All currents were measured 20 msec after beginning of clamp pulse. Abscissa: internal potential during pulse.

Fig. 12 shows the current-voltage relations for the tetrodotoxin-sensitive current with 25 mM-CsF + sucrose inside (○) and with 6 mM-NaF + 19 mM-CsF + sucrose inside (●). They were obtained by subtracting the tetrodotoxin-insensitive current in column *C* of Fig. 11 from the current in column *A* and column *B*, respectively, assuming that the tetrodotoxin-

insensitive current is not significantly altered by the change of the perfusion fluid.

In Fig. 12 the reversal potential of the tetrodotoxin-sensitive current was $V_e = +60.5$ mV with 25 mM-CsF + sucrose inside and $V_e = +24$ mV with 6 mM-NaF + 19 mM-CsF + sucrose inside. The reversal potentials of seven fibres perfused with 6 mM-NaF + 19 mM-CsF + sucrose or 3 mM-NaF + 22 mM-CsF + sucrose are collected in Table 4A and B. They were determined either by subtracting the tetrodotoxin-insensitive current or by subtracting a linear leakage current. Most of the fibres in Table 4A and B showed a small net inward current when perfused with the NaF + CsF mixture. Comparison of Tables 3 and 4A and B clearly demonstrates that the reversal potential of the tetrodotoxin-sensitive current is much smaller with a mixture of NaF + CsF as internal solution than with CsF alone.

TABLE 4. Effect of internal and external sodium on reversal potential V_e of tetrodotoxin-sensitive current

(A) 3 mM-NaF + 22 mM-CsF inside, 100 mM-CaCl ₂ outside		(B) 6 mM-NaF + 19 mM-CsF inside, 100 mM-CaCl ₂ outside	
Axon	V_e	Axon	V_e
26	24 mV	25	21 mV
27	27.5	26	20
28*	24.5	29*	17
Average	25.3	34*	24
S.E.	± 1.1	Average	20.5
		S.E.	± 1.4

(C) 25 mM-CsF inside, 100 mM-CaCl ₂ with 0–50 mM-NaCl outside					
Axon	0 mM-NaCl	5 mM-NaCl	10 mM-NaCl	25 mM-NaCl	50 mM-NaCl
19*	$V_e = 57$	$V_e = 64.5$ mV	—	—	—
21*	= 61	—	$V_e > 67$ mV	—	—
18*	= 48.5	—	—	$V_e = 73.5$ mV	—
13	= 39.5	—	—	—	$V_e = 77$ mV

Temperature 16.0–17.0° C. Isotonicity of solutions maintained with sucrose.

* V_e determined from clamp runs without and with tetrodotoxin; in the other experiments V_e was obtained from leakage correction using hyperpolarizing pulses.

Fig. 12 provides a further argument against the idea that the inward current is carried by sodium ions left behind in the extracellular space. If the inward current were carried by Na, a reversal potential of 24 mV as found for 6 mM-NaF + 19 mM-CsF inside would correspond to an extracellular Na concentration of $6 \times \text{antilog}(24/57.3) = 15.7$ mM which would be an unreasonably high value.

Further experiments were done with a Na salt alone as internal electrolyte, using 25 mM-NaF + sucrose or Na phosphate + sucrose with 15 mM-Na as perfusion fluid. Two experiments of this kind are illustrated in Fig. 13 *A* and *B*. The current records with Na phosphate + sucrose (containing 15 mM-Na) inside were very similar to those with 6 mM-NaF + 19 mM-CsF + sucrose in column *B* of Fig. 11. They showed no net inward current and a fairly large outward current at moderate depolarizations. In one of these two experiments (Fig. 13*A*) the membrane current was split into its two com-

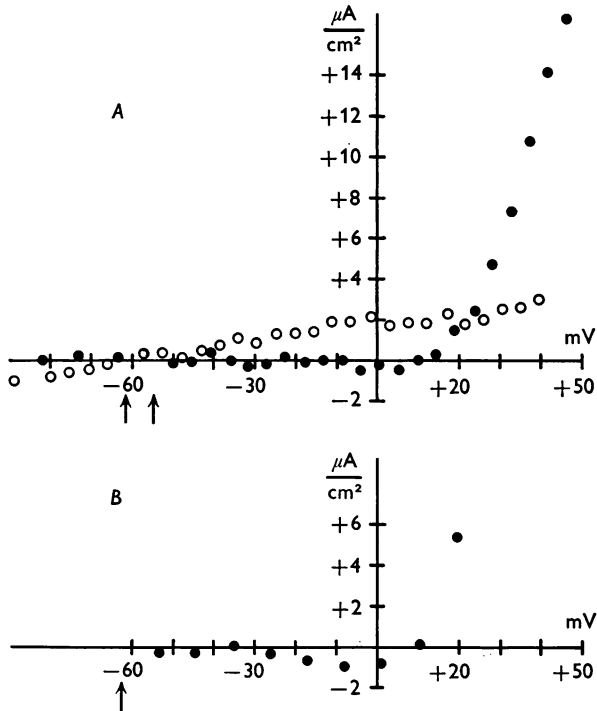


Fig. 13. Current-voltage relation with 15 mM-Na in the internal solution. Two different experiments, both with 100 mM-CaCl₂ + sucrose outside and Na phosphate (containing 15 mM-Na) + sucrose inside. Holding potentials indicated by arrows. All currents were measured 10 msec after beginning of clamp pulse. Abscissa: internal potential during pulse. *A*: ●, Tetrodotoxin-sensitive current = (current before application of tetrodotoxin) - (current after application of tetrodotoxin); ○, tetrodotoxin-insensitive current = current after application of tetrodotoxin. The currents before application of tetrodotoxin were recorded with a holding potential of -54.5 mV and a resting potential of -24.5 mV. The currents after application of tetrodotoxin were recorded 21 min after adding tetrodotoxin (final concentration 1.5 μM), holding potential -61.5 mV, resting potential -6.5 mV. Axon 24, diameter 750 μm. Temperature 16° C. *B*: ●, Current corrected for leakage current. Holding potential -62.5 mV, resting potential -22.5 mV. Axon 22, diameter 700 μm. Temperature 17° C.

ponents, the tetrodotoxin-sensitive current (●) and the tetrodotoxin-insensitive current (○). The latter followed almost a straight line (slope $27.3 \text{ k}\Omega \text{ cm}^2$) whereas the measurements of the tetrodotoxin-sensitive current (●) seem to suggest a very small inward current around 0 mV. In the other experiment (Fig. 13*B*) an approximate estimate of the tetrodotoxin-sensitive current was obtained by subtracting a linear leakage current. The resulting points (●) again suggest a weak inward current in the region of 0 mV. The reversal potential of the tetrodotoxin-sensitive current was estimated from Fig. 13*A* and *B* to be about +9.5 to +10 mV.

Fibres perfused with a Na salt or a Na+Cs mixture responded to moderate depolarizations with a fairly large outward current (see records 28.5 and 37.5 mV in Fig. 11*B*). Plotting the tetrodotoxin-sensitive part of the outward current on semilogarithmic paper revealed an exponential decline during the first 20 or 30 msec (time constants 15 to 25 msec for internal potentials between +10 and +50 mV), followed by a much slower decay; for instance, at the end of the 60 msec pulse to 37.5 mV in Fig. 11*B* the tetrodotoxin-sensitive outward current was still $6 \mu\text{A}/\text{cm}^2$. The general time course of the tetrodotoxin-sensitive Na outward current is similar to that of the tetrodotoxin-sensitive Ca inward current measured in the same potential range (see p. 235). This gives further support to the idea that both ions go through the same channel.

Effect of external Na on membrane currents

Adding small amounts of NaCl to the external 100 mM-CaCl₂+sucrose solution increased the tetrodotoxin-sensitive inward current and its reversal potential. Fairly unexpected was the finding that the time course of the Na inward current is different from the time course of the Ca inward current. The effects of external Na are described in Table 4*C* and Figs. 14–16.

Table 4*C* shows the effect of external Na on the reversal potential V_e of the tetrodotoxin-sensitive current. For each of the four fibres V_e in 100 mM-CaCl₂+sucrose without NaCl (compare Table 3) and V_e in 100 mM-CaCl₂+sucrose with 5–50 mM-NaCl are given. The latter values were measured 11–21 min after adding NaCl to the external solution. They are clearly larger than the reversal potentials in Na-free solution. A fifth experiment which indicated an even larger shift of the reversal potential (from +47 mV in 100 mM-CaCl₂ to +91 mV in 100 mM-CaCl₂+37.5 mM-NaCl) has not been included in the Table. Adding external NaCl increased the maximum tetrodotoxin-sensitive inward current by a factor of 1.16 in axon 19 (5 mM-NaCl added) and by a factor of 5.8 in axon 18 (25 mM-NaCl added). Axon 13 fired spontaneous action potentials of about 80 mV amplitude and 20 sec duration in the solution containing 50 mM-NaCl.

Fig. 14 illustrates the three effects of adding NaCl to the external solution, namely the increase in inward current, the change in reversal potential and the change in the time course of the currents. With 100 mM-CaCl₂ + sucrose outside (column *A*) the currents had their usual appearance: a small and slowly decaying inward current for small depolarizations, a change to outward current at stronger depolarizations and a marked increase of the outward current at even stronger depolarizations. The reversal potential as estimated by subtracting a linear leakage current was $V_e = +39.5$ mV in column *A* (see Table 4*C*). Records in 100 mM-CaCl₂ +

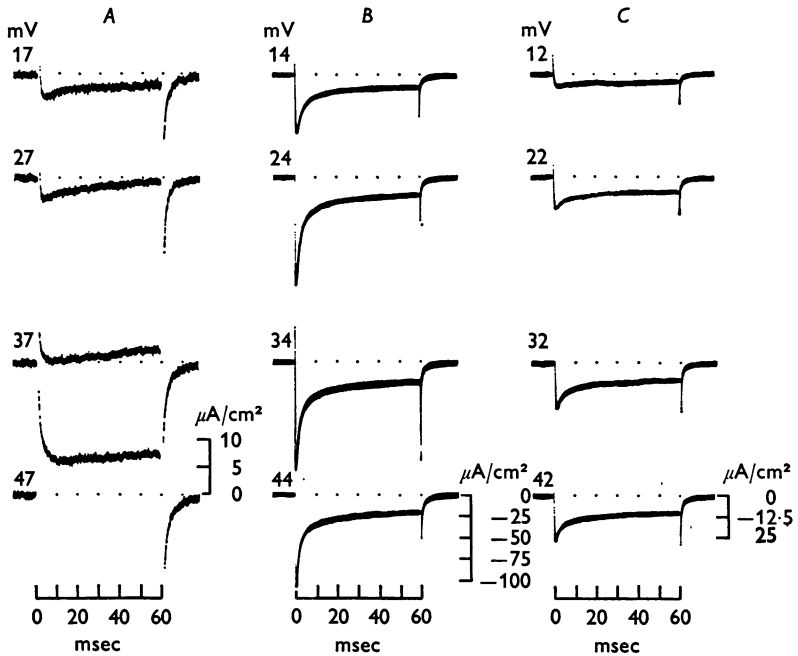


Fig. 14. Effect of external Na on membrane currents. *A*: 100 mM-CaCl₂ + sucrose outside, resting potential = holding potential = -33 mV. *B*: 100 mM-CaCl₂ + 50 mM-NaCl + sucrose outside, resting potential -16 mV, holding potential -36 mV. *C*: 100 mM-CaCl₂ + 50 mM-NaCl + sucrose outside, resting potential = holding potential = -18 mV. Internal solution: 25 mM-CsF + sucrose. Note different current gains. Records were taken in the sequence *A*, *C*, *B*. Axon 13, diameter 650 μm . Temperature 16.7° C.

sucrose + 50 mM-NaCl (column *B*) were taken on a six times lower gain and show a large inward current over the whole potential range. With stronger voltage clamp pulses (not shown in Fig. 14) the reversal potential was determined as $V_e = +77$ mV. Measurements of V_e were started 12 min after adding the NaCl and were repeated several times during the

following 31 min, giving always the same result within 5 mV; we therefore feel confident that the NaCl had properly reached the membrane.

The time course of the inward current in column *B* is different from that in column *A*. It shows a pronounced initial peak from which the current rapidly decayed to a maintained level. Inward currents with an initial peak were also seen with 10 or 25 mM-NaCl in the external solution (axons 21 and 18 in Table 4*C*), but not with 5 mM-NaCl (axon 19). The peak seemed to become more pronounced with increasing NaCl concentration. The records in Fig. 7*B* which were taken in 100 mM-MgCl₂ + sucrose + 20 mM-NaCl also show the initial peak.

Records in Fig. 14*A* and *B* were taken at almost the same holding potential (−33 and −36 mV, respectively) whereas in *C* the holding potential was only −18 mV. The currents in *C*, although recorded with the same external solution as those in *B*, have almost completely lost the fast initial peak. Their time course is rather similar to that of the much smaller inward currents in Na-free solution which are shown in the two uppermost records of *A*.

The magnitude and time course of the currents are illustrated more clearly by Fig. 15 which presents semilogarithmic plots of three current records from Fig. 14, namely those labelled 27 mV in column *A*, 24 mV in column *B* and 22 mV in column *C*. A few values from records on a five times faster time base are also included in Fig. 15*A*. The current in *B* (100 mM-CaCl₂ + sucrose + 50 mM-NaCl) is clearly larger than the currents in *C* (same solution, low holding potential) and *A* (100 mM-CaCl₂ + sucrose without NaCl). Also, the current in *B* consists of two components, an initial fast one and a second slower component. The time constant of the fast component (= total current – extrapolated slow component) was 2.5 msec and that of the slow component 13.6 msec. In *C* and *A* the fast component is much smaller or absent whereas the slow component ($\tau = 13.75$ msec in *C* and 14.4 msec in *A*) is still present although smaller than in *B*. We have never seen a clear fast component in 100 mM-CaCl₂ without NaCl, even in experiments with fairly high holding potentials such as −47 mV in Fig. 9*B* or −50 mV in Fig. 8*C*.

The experiment in Figs. 14 and 15 shows that the fast initial peak of Na inward current is more sensitive to inactivation than the slow current component. Another experiment in which the height of the depolarizing clamp pulse was varied in small steps indicated that the slow current component turns on at a slightly smaller depolarization than the fast initial peak. These findings could be interpreted by assuming that there are two types of tetrodotoxin-sensitive channels, slow channels which have a fairly high permeability for both Na and Ca ions and fast channels which are mainly used by Na ions. An important conclusion

from the experiment in Figs. 14 and 15 is that the ratio I_{Ca}/I_{Na} is time dependent during the first 5 msec, suggesting a time dependence of the permeability ratio P_{Ca}/P_{Na} . According to Fig. 15 the ratio P_{Ca}/P_{Na} would be small at short times and larger at longer times. A further observation which supports the idea of a time dependent permeability ratio P_{Ca}/P_{Na} is discussed on p. 258.

Time constants were also determined for the other current records in Fig. 14. All the currents in column *B* consisted of two components, a fast and a slow; the currents in column *A* and *C* showed practically only the

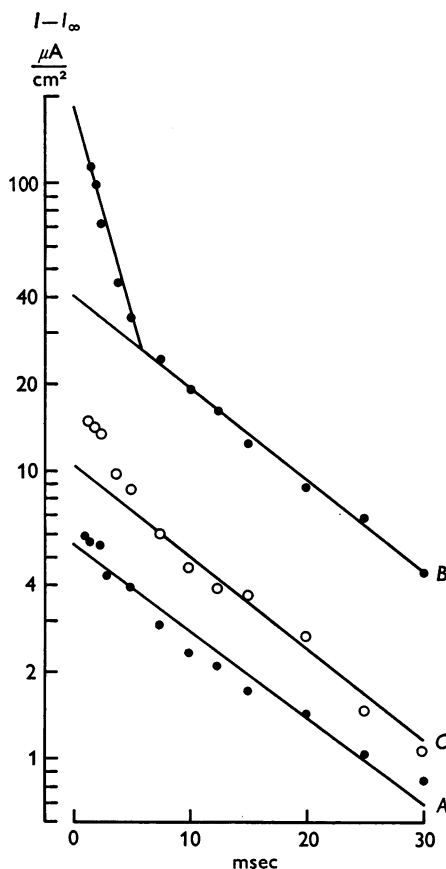


Fig. 15. Semilogarithmic plot of some of the currents from Fig. 14. *A*: ●, record 27 mV from Fig. 14*A*. *B*: ●, record 24 mV from Fig. 14*B*. *C*: ○, record 22 mV from Fig. 14*C*. Abscissa: time after beginning of clamp pulse. Ordinate: $(I - I_{\infty})$ on a logarithmic scale where I_{∞} is the current at the end of the 60 msec clamp pulse. All currents have been corrected for capacity and (linear) leakage current. The straight lines represent the following time constants: 14.4 msec in *A*, 2.5 and 13.6 msec in *B*, 13.75 msec in *C*.

slow component. The time constant of the fast component (= total current - extrapolated slow component) varied between 1.5 and 2.5 msec for internal potentials between +14 and +64 mV; increasing depolarization seemed to reduce the time constant. The time constant of the slow component as determined from the records in columns *A*, *B* and *C* was 11 msec at +14 mV; it increased with increasing depolarization and

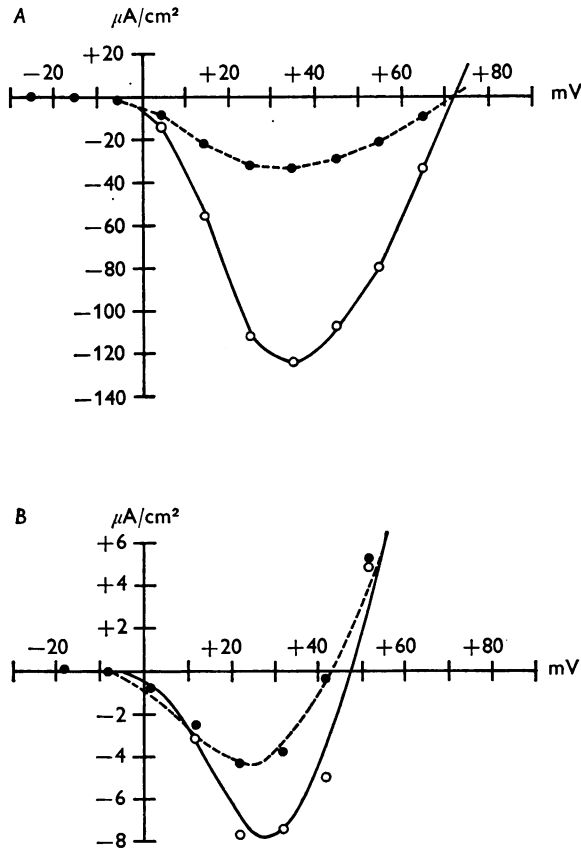


Fig. 16. Effect of external Na on current-voltage relation. Same experiment as in Figs. 14 and 15. The currents are from clamp runs on a five times faster time base than those in Fig. 14. *A*: 100 mM-CaCl₂ + 50 mM-NaCl + sucrose outside, resting potential -15 mV, holding potential -35 mV; ○, current at peak; ●, current 12 msec after beginning of clamp pulse. *B*: 100 mM-CaCl₂ + sucrose without NaCl outside, resting potential = holding potential = -28 mV; ○, current measured at the same time as the peak current in *A*; ●, current 12 msec after beginning of clamp pulse. All currents corrected by subtracting capacity current and linear leakage current. Note different ordinate scales in *A* and *B*. Curves in *A* drawn by eye. Curves in *B* calculated from curves in *A* by means of eqn. (10) with values for V_{e1} , V_{e2} , y_{01} and y_{02} as given in text on p. 258.

became 26 msec at +64 mV. Similar time constants for the slow decline of the Ca inward current or Na outward current during the first 20–30 msec have been given on pp. 235 and 247.

The effect of external Na on the membrane currents is further illustrated by Fig. 16. The data in Fig. 16 are from the same experiment as Figs. 14 and 15, but from clamp runs on a faster time base. The measuring points in Fig. 16*A* are the peak currents (○) and the 12 msec currents (●) in 100 mM-CaCl₂ + sucrose + 50 mM-NaCl. Fig. 16*B* gives the corresponding measuring points for 100 mM-CaCl₂ + sucrose without NaCl. Since there were no clear current peaks in the latter solution, the points ○ in *B* represent the currents measured at the same time as the peak currents in *A*, i.e. 1–2 msec after the beginning of the clamp pulse. Comparison of *A* and *B* confirms the findings from Figs. 14 and 15. The currents were much larger in the presence of 50 mM-NaCl (*A*) than in the Na-free medium (*B*). The ratio 12 msec current:peak current was smaller in *A* than in *B*, as expected from the rapid initial decay of the Na current. The reversal potential was +72 mV in *A* and +42.5 to +47 mV in *B* which is in satisfactory agreement with the values +77 mV and +39.5 mV mentioned in the discussion of Fig. 14. The main objective of the experiment in Fig. 16 was to find out whether the currents in *B* could be predicted from those in *A* by application of the independence principle (Hodgkin & Huxley, 1952*a*). Two curves were drawn by eye through the experimental points in *A*. From the two curves in *A* we calculated the two curves in *B* by means of the independence principle. They are clearly a satisfactory fit to the experimental points in *B*. Possible conclusions from Fig. 16 are discussed on p. 258 where details of the calculation are given.

The peak currents (○) in Fig. 16*A* were also used to calculate the voltage dependence of the Na permeability P_{Na} . The permeability P_{Na} was obtained from the constant field equation for I_{Na} ; the equation for I_{Na} was identical to eqn. (2) for I_{Ca} (see p. 253), assuming $V' = 0$. The relation between P_{Na} and internal potential V was steepest between +5 and +15 mV with a limiting slope corresponding to an e-fold increase in P_{Na} for a change of about 6 mV. The voltage at which P_{Na} reached 0.1 ($P_{\text{Na}}\text{max}$) was +11 mV as compared with -40 to -45 mV for fibres perfused with 300 mM-NaF + sucrose (see Fig. 9 of Chandler & Meves, 1970*a*). This indicates a shift of +50 to +55 mV. From Table 3 of Chandler, Hodgkin & Meves (1965) a shift of +34 mV is expected for lowering the internal salt concentration from 300 to 24 mM; an additional shift of about +10 mV will be caused by the high external Ca. The negative resistance branch of the peak Na current curve in Fig. 16*A* is similar in position to that of the curve for the tetrodotoxin-sensitive Ca inward current in Figs. 4, 10 and 12.

Calculation of the permeability ratios P_{Ca}/P_{Cs} , P_{Ca}/P_{Na} and P_{Cs}/P_{Na}

The main experimental findings can be summarized as follows. With 100 mM-CaCl₂ outside and 25 mM-CsF inside tetrodotoxin-sensitive Ca inward currents were seen in the potential range between 0 and +50 to +60 mV. Larger depolarizations caused an outward current which was partly blocked by tetrodotoxin. The tetrodotoxin-sensitive outward current was not abolished by a Cl-free external medium and is probably carried by Cs ions moving through the Na channel. At the reversal potential of the tetrodotoxin-sensitive current the Ca current I_{Ca} and the Cs current I_{Cs} are equal and opposite. The average value of the reversal potential was found to be +54.1 mV at 15.8–17.0° C.

Mathematical expressions for the currents I_{Ca} and I_{Cs} were obtained from the constant field equations (Goldman, 1943; Hodgkin & Katz, 1949). The equations were modified by assuming fixed negative charges at the inside of the membrane. This modification was suggested to us by Professor Sir Alan Hodgkin. It was first introduced by Frankenhaeuser (1960) to account for the fact that the $I_{Na}-V$ curve in squid axons is linear at large values of V . The effect of fixed charges is equivalent to a variation of the partition coefficient through the membrane. With a potential step V' at the inside of the membrane the equation for the Cs current (see eqn. (5) of Frankenhaeuser, 1960) becomes

$$I_{Cs} = P_{Cs} \frac{(V - V')F^2}{RT} [Cs]_o \frac{\exp((V - V_{Cs})F/RT) - 1}{\exp((V - V')F/RT) - 1} \quad (1)$$

$$= P_{Cs} \frac{(V - V')F^2}{RT} \frac{[Cs]_i \exp(V'F/RT) - [Cs]_o \exp(-(V - V')F/RT)}{1 - \exp(-(V - V')F/RT)} \quad (2)$$

The corresponding equations for the Ca current are

$$I_{Ca} = 4P_{Ca} \frac{(V - V')F^2}{RT} [Ca]_o \frac{\exp(2(V - V_{Ca})F/RT) - 1}{\exp(2(V - V')F/RT) - 1} \quad (3)$$

$$= 4P_{Ca} \frac{(V - V')F^2}{RT} \frac{[Ca]_i \exp(2V'F/RT) - [Ca]_o \exp(-2(V - V')F/RT)}{1 - \exp(-2(V - V')F/RT)} \quad (4)$$

$[Cs]_o$, $[Cs]_i$, $[Ca]_o$ and $[Ca]_i$ are the activities of Cs and Ca in the external and internal solution, P_{Cs} and P_{Ca} are the Cs and Ca permeabilities of the Na channel and R , T and F have their usual meanings.

For $[Cs]_o = [Ca]_i = 0$, $V = V_e$ and $I_{Cs} = -I_{Ca}$ eqns. (2) and (4) lead to

$$4 \frac{P_{Ca} [Ca]_o}{P_{Cs} [Cs]_i} = \exp(V_e F/RT) [\exp((V_e - V') F/RT) + 1]. \quad (5)$$

We assumed V' to be large and positive. This assumption was made for simplicity; the alternative assumptions $V' = +50$ mV or $V' = 0$ mV do not substantially alter our main conclusions (see p. 262). For large and positive V' the term in [] approaches unity and V_e is obtained as

$$V_e = 57.3 \log \frac{4P_{Ca} [Ca]_o}{P_{Cs} [Cs]_i} \quad (6)$$

at 16° C. This equation predicts a 57.3 mV change in V_e for a tenfold change in $[Ca]_o$. This is in agreement with Fig. 13 of Fatt & Ginsborg (1958) which in the range of large negative internal potentials indicates a 57.3 mV change per tenfold change in divalent cation concentration.

According to eqn. (6) the change from 100 to 200 mM-CaCl₂ + sucrose (corresponding to $[Ca]_o = 35.5$ and 51 m-mole/kg H₂O) should increase V_e by 9 mV; this is roughly consistent with the two experiments described on page 242 which gave $\Delta V_e = 10.5$ and 14 mV. For comparison the theoretical values of ΔV_e were also calculated for $V' = +50$ mV (which is the fixed charge potential for 25 mM internal salt concentration estimated from Table 3 of Chandler, Hodgkin & Meves, 1965) and for $V' = 0$ mV; the values obtained from eqn. (5) under these assumptions are $\Delta V_e = 5.5$ and 4.5 mV, respectively, and are clearly smaller than the experimental ΔV_e . For the change from 10 to 100 mM-CaCl₂ (corresponding to $[Ca]_o = 5$ and 35.5 m-mole/kg H₂O) the experimentally observed ΔV_e was 22.5 and 22 mV (see p. 242). This change in reversal potential corresponds almost to a 29 mV slope and is close to the theoretical value of $\Delta V_e = 26.5$ mV predicted from eqn. (5) under the assumption $V' = 0$ mV. Thus, the experimental results in high external Ca are best fitted by the assumption $V' \gg V_e$ whereas those in low external Ca seem to require $V' = 0$ mV. It is difficult to assess the significance of this observation because the measurements of ΔV_e may not be sufficiently accurate. A tentative explanation would be that the effect of internal fixed negative charges is compensated in low external Ca by the unmasking of negative surface charges at the outside of the membrane.

With eqn. (6) and the ion activities from Tables 1 and 2 the average value of $V_e = +54.1$ mV measured with 100 mM-CaCl₂ + sucrose outside and 25 mM-CsF + sucrose inside (Table 3A) leads to a permeability ratio $P_{Ca}/P_{Cs} = 1/0.62$. For $V_e = +50$ or $+60$ mV the permeability ratio is 1/0.73 or 1/0.49.

If $P_{Na} [Na]_i$ is substituted for $P_{Cs} [Cs]_i$, eqn. (6) can be used to calculate P_{Ca}/P_{Na} from V_e measurements on fibres with internal Na. In the two experiments of Fig. 13 the internal solution was Na phosphate + sucrose with 15 mM-Na and the reversal potential was estimated as $+9.5$ to $+10$ mV, corresponding to a permeability ratio $P_{Ca}/P_{Na} = 1/6.9$.

With the three ions Cs^+ , Ca^{2+} and Na^+ present (i.e. NaCl added to the external solution or part of the internal CsF replaced by NaF) eqn. (6) has to be replaced by

$$\begin{aligned} V_e &= 57.3 \log \frac{(P_{\text{Na}}/4P_{\text{Ca}}) [\text{Na}]_o + [\text{Ca}]_o}{(P_{\text{Na}}/4P_{\text{Ca}}) [\text{Na}]_i + (P_{\text{Cs}}/4P_{\text{Ca}}) [\text{Cs}]_i} \\ &= 57.3 \log \frac{[\text{Na}]_o + (4P_{\text{Ca}}/P_{\text{Na}}) [\text{Ca}]_o}{[\text{Na}]_i + (P_{\text{Cs}}/P_{\text{Na}}) [\text{Cs}]_i} \end{aligned} \quad (7)$$

at 16°C . Eqn. (7) is derived in the same way as eqn. (6).

In the experiment of Fig. 12 the reversal potential was $V_e = +60.5 \text{ mV}$ with 25 mm- CsF inside and $V_e = +24 \text{ mV}$ with 6 mm- NaF + 19 mm- CsF inside. The first value and eqn. (6) give $P_{\text{Ca}}/P_{\text{Cs}} = 1/0.48$; this ratio, the value $V_e = +24 \text{ mV}$ and eqn. (7) lead to $P_{\text{Ca}}/P_{\text{Na}} = 1/6.9$ which is identical with the ratio deduced from Fig. 13.

The experiments in Table 4C gave a reversal potential for 25 mm- CsF inside and 100 mm- CaCl_2 outside (leading to a permeability ratio $P_{\text{Ca}}/P_{\text{Cs}}$ as calculated from eqn. (6)) and a reversal potential for 100 mm- CaCl_2 + NaCl outside. From the latter reversal potential and the ratio $P_{\text{Ca}}/P_{\text{Cs}}$ we calculated the permeability ratio $P_{\text{Ca}}/P_{\text{Na}}$ by means of eqn. (7). In this way the following permeability ratios $P_{\text{Ca}}/P_{\text{Na}}$ were found from the experiments listed in Table 4C: 1/8.4 from axon 19, 1/9.7 from axon 18, 1/10.1 from axon 13.

The conclusion from the experiments in Figs. 13 and 12 and in Table 4C is that $P_{\text{Ca}}/P_{\text{Na}}$ is between 1/10 and 1/7 under our experimental conditions. The validity of these estimates is necessarily uncertain; our values for $P_{\text{Ca}}/P_{\text{Na}}$ depend on the use of the constant field equation for the interpretation of the experimental results.

From the two ratios $P_{\text{Ca}}/P_{\text{Cs}} = 1/0.62$ and $P_{\text{Ca}}/P_{\text{Na}} = 1/10$ to $1/7$ follows the ratio $P_{\text{Cs}}/P_{\text{Na}} = 1/16$ to $1/11$. A direct determination of the permeability ratio $P_{\text{Cs}}/P_{\text{Na}}$ is possible by measuring the reversal potential of the tetrodotoxin-sensitive current in a situation where we have Na inward current, but no Ca inward current (Fig. 7B with 100 mm- MgCl_2 + sucrose + 20 mm- NaCl as external solution) or comparatively little Ca inward current (Fig. 16A with 100 mm- CaCl_2 + sucrose + 50 mm- NaCl). The reversal potential V_e and the permeability ratio $P_{\text{Cs}}/P_{\text{Na}}$ are related by the equation

$$V_e = 57.3 \log \frac{P_{\text{Na}} [\text{Na}]_o}{P_{\text{Cs}} [\text{Cs}]_i} \quad (8)$$

at 16°C . This equation is valid independent from the existence of a potential step V' . In both experiments (Figs. 7B and 16A) the reversal potential was determined by subtracting a linear leakage because a voltage clamp

run with tetrodotoxin was not available. We obtained $V_e = +73.5$ mV and $+58$ mV (Fig. 7B, two clamp runs) and $V_e = +72$ mV (Fig. 16A), corresponding to permeability ratios $P_{Cs}/P_{Na} = 1/22.6$, $1/12.1$ and $1/9.2$.

Values for the reversal potential V_e , obtained under varying experimental conditions, are collected in Table 5. The ion activities in the external and internal solutions as determined with ion-selective electrodes (Tables 1 and 2) are also given. From the measured ion activities and the

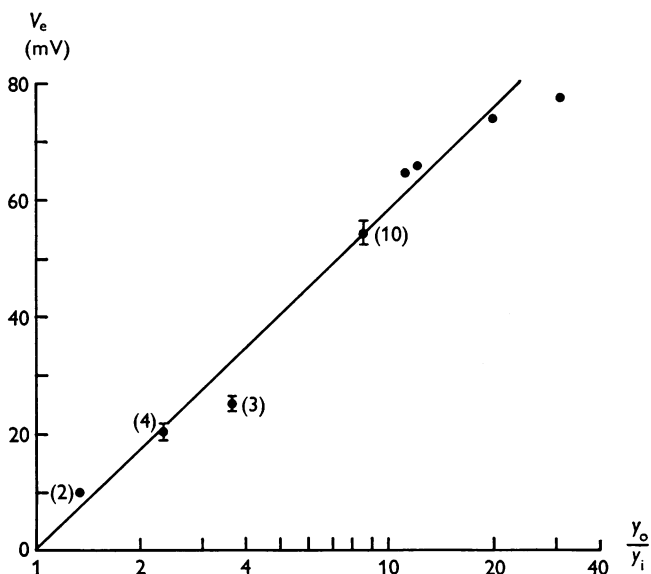


Fig. 17. Reversal potential of the tetrodotoxin-sensitive current under different experimental conditions. Ordinate: reversal potential V_e . Abscissa: activity ratio y_o/y_i , calculated from eqn. (9a) and (9b) with $P_{Ca}/P_{Na} = 1/7.5$ and $P_{Cs}/P_{Na} = 1/12$, on a logarithmic scale. The points are from Table 5; number of experiments indicated. The vertical bars represent \pm s.e. The straight line was drawn with a slope of 57.3 mV per tenfold change in y_o/y_i .

permeability ratios $P_{Ca}/P_{Na} = 1/7.5$ and $P_{Cs}/P_{Na} = 1/12$ we calculated apparent sodium activities y_o and y_i of the external and internal solutions. According to eqn. (7) they are defined as

$$y_o = [Na]_o + (4P_{Ca}/P_{Na}) [Ca]_o, \quad (9a)$$

$$y_i = [Na]_i + (P_{Cs}/P_{Na}) [Cs]_i. \quad (9b)$$

In Fig. 17 the experimental values for V_e are plotted against $\log y_o/y_i$. A straight line is drawn with a slope of 57.3 mV per tenfold change in y_o/y_i . It fits the points satisfactorily, indicating that the reversal potential

TABLE 5. Reversal potential V_e of the tetrodotoxin-sensitive current under varying experimental conditions

External solution	[Ca] _o	[Na] _o	%	Internal solution	[Cs] _i	[Na] _i	y ₁	y ₀ /y ₁	V _e (mV)	Source	No. of experiments
100 mM-CaCl ₂	35.5	—	18.96	Na phosphate with 15 mM-Na	—	14	14	1.35	9.75	Fig. 13	2
100 mM-CaCl ₂	35.5	—	18.96	6 mM-NaF + 19 mM-CsF	19.5	6.5	8.12	2.34	20.5	Table 4B	4
100 mM-CaCl ₂	35.5	—	18.96	3 mM-NaF + 22 mM-CsF	22.75	3.25	5.15	3.68	25.3	Table 4A	3
100 mM-CaCl ₂	35.5	—	18.96	25 mM-CsF	26	—	2.17	8.74	54.1	Table 3A	10
200 mM-CaCl ₂	51	—	27.20	25 mM-CsF	26	—	2.17	12.53	65.5	Fig. 10	1
100 mM-CaCl ₂ + 5 mM-NaCl	35.5	6	24.96	25 mM-CsF	26	—	2.17	11.49	64.5	Table 4C	1
100 mM-CaCl ₂ + 25 mM-NaCl	33	26.5	44.12	25 mM-CsF	26	—	2.17	20.3	73.5	Table 4C	1
100 mM-CaCl ₂ + 50 mM-NaCl	31.5	51	67.80	25 mM-CsF	26	—	2.17	31.2	77	Table 4C	1

[Ca]_o, [Na]_o, [Cs]_i, [Na]_i are measured activities in m-mole/kg H₂O (see Tables 1 and 2). y₀ and y₁ are the apparent Na activities of the external and internal solutions as calculated from eqn. (9a) and (9b) with $P_{Ca}/P_{Na} = 1/7.5$ and $P_{Ca}/P_{Na} = 1/12$. Isotonicity of the solutions maintained with sucrose. Temperature 15.8–17.0° C.

V_e is correctly described by eqn. (7) and the permeability ratios $P_{Ca}/P_{Na} = 1/7.5$ and $P_{Cs}/P_{Na} = 1/12$. Our results can thus be summarized by saying that under our experimental conditions the Na channel is still primarily permeable to Na ions. Its selectivity, however, is comparatively small (see Discussion).

Our permeability ratios are consistent with the observation of Tasaki, Lerman & Watanabe (1969) that for $[Na]_o > 100$ mM the action potential overshoot follows $[Na]_o$ with a 58 mV slope. Eqn. (7) with $P_{Ca}/P_{Na} = 1/7.5$ and $P_{Cs}/P_{Na} = 1/12$ predicts $\Delta V_e = 15$ mV for changing from 100 mM-CaCl₂ + 100 mM-NaCl to 100 mM-CaCl₂ + 200 mM-NaCl and $\Delta V_e = 5$ mV for changing from 100 mM-CaCl₂ + 5 mM-NaCl to 100 mM-CaCl₂ + 10 mM-NaCl; the theoretical ΔV_e for a 58 mV slope would be 17 mV.

The conclusion that P_{Ca}/P_{Na} is 1/10 to 1/7 under our experimental conditions was further tested in Fig. 16. From the currents I_1 measured in 100 mM-CaCl₂ + 50 mM-NaCl (Fig. 16*A*) we calculated the currents I_2 in 100 mM-CaCl₂ without NaCl (Fig. 16*B*), using the independence principle (Hodgkin & Huxley, 1952*a*) and appropriate values for P_{Ca}/P_{Na} . The independence principle predicts the ratio

$$\frac{I_2}{I_1} = \frac{y_{o2} [\exp((V - V_{e2}) F/RT) - 1]}{y_{o1} [\exp((V - V_{e1}) F/RT) - 1]}, \quad (10)$$

where V_{e1} and V_{e2} are the reversal potentials of the tetrodotoxin-sensitive current and y_o is the apparent sodium activity of the external solution as defined by eqn. (9*a*). V_{e1} and V_{e2} were estimated as +72 mV and +42.5 to 47 mV respectively (see p. 252). The two curves in *A* were drawn by eye through the measuring points for the peak currents (○) and for the currents at 12 msec (●). The two curves in *B* were calculated from eqn. (10), using I_1 as read from the two curves in *A* and y_o as calculated from eqn. (9*a*). For the latter step we used the measured activities $[Na]_o$ and $[Ca]_o$ (see Tables 1 and 2) and permeability ratios P_{Ca}/P_{Na} between 1/25 and 1/7.5. The best fits were obtained with 1/25 for the peak currents (○) and 1/10 for the 12 msec currents (●) and the two curves in part *B* are drawn with these permeability ratios. The ratio 1/10 did not give a good fit for the peak currents, the predicted currents being more than twice too large.

The experiment of Fig. 16 thus confirms the conclusion that the permeability ratio P_{Ca}/P_{Na} , determined from the tetrodotoxin-sensitive currents measured 10–20 msec after the beginning of the clamp pulse, is in the order of 1/10. It also suggests that the ratio is smaller for shorter times, namely for the first 1–2 msec after the beginning of the clamp pulse; this supports the conclusion reached in the discussion of Fig. 15 (see p. 250).

DISCUSSION

The experiments have shown that inward currents carried by Ca ions can be recorded from the squid giant axon under suitable experimental conditions. The Ca inward currents can produce action potentials in the absence of external Na as first described by Tasaki *et al.* (1966, 1967). The inward currents were completely abolished by tetrodotoxin. Tetrodotoxin-insensitive Ca inward currents, corresponding to the late Ca entry in aequorin experiments on intact axons (Baker *et al.* 1971), have not been observed. A possible explanation would be that the late Ca entry seen with aequorin represents an electroneutral exchange.

The net inward currents were only 4–6 $\mu\text{A}/\text{cm}^2$ in size. It was important to exclude the possibility that these small currents are carried by residual Na ions, left behind in the space between the small nerve fibres which surround the giant axon. The following observations argue against this possibility. (1) There was no inward current with 100 mM-MgCl₂ + sucrose as external solution (Figs. 7A, 8A), although the fibres were fully excitable as shown by the inward currents recorded in 100 mM-MgCl₂ + sucrose + 20 mM-NaCl (Fig. 7B). (2) There was no significant correlation between the reversal potential of the tetrodotoxin-sensitive current and the time spent in Na-free solution (see p. 235). (3) Adding 5 mM-NaCl to the external 100 mM-CaCl₂ + sucrose solution had only a small effect on the size of the inward current and on the reversal potential (see p. 247 and Table 4C). (4) A small inward current was seen with 6 mM-NaF + 19 mM-CsF + sucrose as internal solution (Fig. 12); if this inward current were carried by Na ions one would have to assume an unreasonably high concentration of residual extracellular Na (see p. 245). (5) The size of our Ca currents is compatible with tracer measurements of Ca entry made by Takenaka & Yumoto (1969) under similar experimental conditions.

Takenaka & Yumoto investigated axons which were perfused with 25 mM-CsF + glycerol and immersed in a solution of 100 mM-CaCl₂ + glycerol. They measured the uptake of ⁴⁵Ca during the long lasting action potentials which are obtained under these conditions. From their data we calculated the ⁴⁵Ca uptake during the action potential as 0.09 p-mole/cm² msec which is close to the value of 0.08 p-mole/cm² for the Ca uptake per action potential in intact axons in sea water with 112 mM-CaCl₂ (Hodgkin & Keynes, 1957). A Ca uptake of 0.09 p-mole/cm² msec corresponds to an electric current of 18 $\mu\text{A}/\text{cm}^2$; this is 2.25 times more than our tetrodotoxin-sensitive inward current which had a maximum of 8 $\mu\text{A}/\text{cm}^2$ (see Figs. 12, 16B).

The Ca inward currents, in spite of their small size, were able to elicit action potentials in fibres perfused with 25 mM-CsF + sucrose. As outlined in the introduction, this is due to two reasons, the slow inactivation of the inward current and the almost complete absence of an outward current. The second point is well illustrated by the small slope of the current-

voltage relation of the tetrodotoxin-insensitive current. The slope corresponded to a membrane resistance of $33 \text{ k}\Omega \text{ cm}^2$ (Fig. 4) or $42 \text{ k}\Omega \text{ cm}^2$ (Fig. 6) over a wide potential range; at potentials larger than $+25$ or $+30 \text{ mV}$ the slope increased slightly, probably due to rectification in the leakage channel (see p. 234). Slow inactivation of the weak Ca inward currents is a necessary condition for obtaining Ca action potentials. An electric charge of $45 \times 10^{-9} \text{ C/cm}^2$ is necessary to alter the potential across the membrane condenser ($0.9 \mu\text{F/cm}^2$) by 50 mV . This requires an inward current of $4 \mu\text{A/cm}^2$ flowing for 11 msec which is the rise time of the Ca action potentials (see p. 230). With the normal rate of Na inactivation the inward current would not flow long enough to elicit an action potential.

The slow inactivation was seen both with Ca inward currents and with Na currents. The Ca currents decayed with a time constant of $10\text{--}20 \text{ msec}$ during the first $20\text{--}30 \text{ msec}$; this was followed by a further, much slower decay. A similar time course was found for the Na outward currents seen with Na phosphate or fluoride in the perfusion fluid. Na inward currents, on the other hand, were characterized by an additional fast component which had a time constant of $1.5\text{--}2.5 \text{ msec}$, lasted about 5 msec and was selectively blocked at low holding potentials; at later times the time course was similar to that of the Ca inward currents and Na outward currents. We have no satisfactory explanation for the finding that the fast initial component is only seen with Na inward currents. A possible, but speculative explanation would be that there are two types of tetrodotoxin-insensitive channels, slow channels which have a high permeability for both Na and Ca ions and fast channels which are preferably used by Na (see p. 249). It should be noted in addition that the Na inward currents which show the fast inactivating component are an order of magnitude larger than the Ca inward or Na outward currents. One might also wonder whether the external Na concentration directly affects the rate of inactivation; this seems, however, unlikely since the inactivation rate constants of 300 mM-NaF -perfused fibres in choline sea water are not different from those in Na sea water (Chandler & Meves, 1970*b*).

Sodium inward currents decaying rapidly from an initial peak to an almost sustained level are illustrated in Figs. 7*B* and 14*B*; they resemble the Na inward currents in fibres perfused with 300 mM-NaF or $\text{CsF} + \text{sucrose}$ (Chandler & Meves, 1970*a*) or with a mixture of Cs_2SO_4 and KF (Adelman & Senft, 1966). Our time constants can be compared with the time constants found in the previous experiments: Chandler & Meves (1970*b*) showed that in axons perfused with $300 \text{ mM-NaF} + \text{sucrose}$ the rate constant β_h is much smaller than in intact axons (Hodgkin & Huxley 1952*b*). Eqn. (6) of Chandler & Meves (1970*b*) predicts $\tau_h = 1/\beta_h = 0.9\text{--}1.5 \text{ msec}$ for potentials between $+10$ and $+60 \text{ mV}$ and a Q_{10} of 3.5 if one assumes that in our experiments the β_h curve is shifted by $+50 \text{ mV}$ along the voltage axis due to the

low ionic strength of the internal solution and the high Ca concentration of the external solution (see p. 252). The predicted values are smaller than the experimental values of 1.5–2.5 msec given above for the initial fast decay of the Na current; a possible explanation is that the low ionic strength of the internal solution increases the time constant of inactivation (Chandler, Hodgkin & Meves, 1965; Adelman, Dyro & Senft, 1965). The time constant of 10–25 msec found for the second slower component of the Na inward currents and for the decay of the Ca inward currents during the first 20–30 msec is difficult to reconcile with previous observations. Chandler & Meves (1970c) described a very slow inactivation process ($\tau = 1-3$ sec at 16–17 °C) which follows the initial fast decay of the Na current in NaF perfused axons. It seems possible that inactivation processes of intermediate rate are interposed between the initial fast and the final slow inactivation (see Adelman & Senft, 1970).

The occurrence of net Ca inward currents or Ca action potentials depends critically on the composition of the internal and external solution. Fibres perfused with 25 mM-CsF + sucrose showed net inward currents in the following three external solutions: 100 or 200 mM-CaCl₂ + sucrose; 10 mM-CaCl₂ + 150 mM-Tris-HCl + sucrose; 11 mM-CaCl₂ + 55 mM-MgCl₂ + sucrose. No net inward currents were seen in Tris sea water with 11 mM-CaCl₂ + 55 mM-MgCl₂, probably due to the much smaller leakage resistance (see p. 243). Tetrodotoxin-sensitive inward currents which exceeded the leakage outward current were also found in some fibres perfused with 100 mM-RbF + 50 mM tetraethylammonium chloride + sucrose and immersed in 100 mM-CaCl₂ + sucrose (H. Meves, unpublished).

The foregoing discussion emphasizes two points. (1) Ca action potentials in squid axons are marginal events which are only obtained under special experimental conditions. (2) The time course of the tetrodotoxin-sensitive Ca inward current observed under these experimental conditions is very slow; it is quite different from the transient time course of the tetrodotoxin-sensitive Ca entry in aequorin-injected intact axons (Baker *et al.* 1971).

Our experimental results are generally consistent with the observations of Tasaki *et al.* (1966, 1967) and Watanabe *et al.* (1967b). The long lasting tetrodotoxin-sensitive action potentials obtained by Tasaki and co-workers with 100 mM-CaCl₂ + glycerol outside and 25 mM-CsF + glycerol inside are well accounted for by the slowly inactivating tetrodotoxin-sensitive Ca inward currents described in this paper. The small size of the net inward currents explains the slow rate of rise of the action potentials.

Our findings differ from those of Tasaki and co-workers in two details: (1) We found a small tetrodotoxin-sensitive inward current but no net inward current in fibres with 100 mM-CaCl₂ outside and 15 mM-Na phosphate inside (p. 246), whereas Watanabe *et al.* (1967a) and Tasaki *et al.* (1969) observed action potentials and net inward currents in fibres perfused with 5–50 mM-Na phosphate or fluoride. (2) We found an increase of the absolute value of the resting potential with increasing [Ca]_o (p. 241) whereas Tasaki *et al.* (1967) report a decrease. It is possible that these discrepancies are due to the different perfusion methods or to differences in the leakage conduct-

ance of the fibres. If the resting potential is determined by the ion activities $[Ca]_o$, $[Cs]_i$ and $[Cl]_o$ and by the relative permeability of the membrane for these ions, changes in external Ca could affect the potential in two different, and possibly opposite, ways, directly through a change in $[Ca]_o$ and indirectly through a change of the relative ion permeability.

The main difference between our work and that of Tasaki and co-workers lies in the interpretation of the experimental results. Tasaki and co-workers conclude that 'the presence of sodium ion externally is not essential for the excitation process' (Watanabe *et al.* 1967*a*) and that 'one has to abandon the assumption that there is a channel specific for sodium ions in the axon membrane' (Watanabe *et al.* 1967*b*). Our conclusion is that even under the special conditions of these experiments the membrane is still primarily permeable to Na ions. A quantitative estimate of the relative permeability of the Na channel for Na^+ and Ca^{2+} led to the permeability ratio $P_{Ca}/P_{Na} = 1/10$ to $1/7$ (see p. 258). The importance of external Na ions for the excitation process is well illustrated by the finding that the size of the Ca inward current is several orders of magnitude smaller than that of the Na inward current; consequently, the maximum rate of rise of the Ca action potentials is 200 times smaller than that of a normal action potential (see p. 231).

The permeability ratio $P_{Ca}/P_{Na} = 1/10$ to $1/7$ is more than 10 times larger than the ratio $1/100$ which Baker *et al.* (1971) deduced from aequorin experiments on intact axons. In comparing the two results it should be remembered that estimates of P_{Ca}/P_{Na} depend on the theory used to interpret the experimental measurements. Baker *et al.* determined the ratio Ca conductance to Na conductance and obtained $g_{Ca}/g_{Na} = 1/100$; from the concentration ratio $[Na]_o/[Ca]_o = 4$ and the proportionality conductance \sim permeability \times concentration \times valency² a permeability ratio $P_{Ca}/P_{Na} = 1/100$ was calculated. Our estimates of the permeability ratio P_{Ca}/P_{Na} were obtained from the reversal potentials of the tetrodotoxin-sensitive current by means of the constant field equation under the assumption of a large fixed negative charge potential V' at the inside of the membrane. Because of the different methods used for estimating P_{Ca}/P_{Na} it is difficult to decide whether the difference between our permeability ratio and that of Baker *et al.* is genuine, i.e. whether the selectivity of the sodium channel under our experimental conditions is smaller than in intact axons.

It can be shown that our comparatively large values for P_{Ca}/P_{Na} are not due to the special assumptions made concerning V' (assumed to be large and positive, see p. 254) and $\gamma_{Ca^{2+}}$ (assumed to be equal to $(\gamma_{CaCl_2})^2$, see p. 229). With $V' = +50$ mV or $V' = 0$ mV even larger permeability ratios are obtained by means of eqn. (5), namely $P_{Ca}/P_{Na} = 1/6$ to $1/5$ for $V' = +50$ mV and $P_{Ca}/P_{Na} = 1/3$ to $1/2$ for $V' = 0$ mV. Using the convention $\gamma_{Ca^{2+}} = \gamma_{CaCl_2}$ instead of $\gamma_{Ca^{2+}} = (\gamma_{CaCl_2})^2$

would increase the Ca activities considerably (see values in brackets in column (4) of Table 2) and would lead to $P_{Ca}/P_{Na} = 1/20$ to $1/14$ which is still appreciably larger than the ratio $1/100$.

Independent evidence for a loss of selectivity under our experimental conditions is provided by the observation that the permeability ratio P_{Cs}/P_{Na} is $1/22$ to $1/9$ in fibres perfused with 25 mM-CsF + sucrose (see p. 256) as opposed to $1/61$ or $1/58$ found previously with 300 mM internal salt concentration and Cl^- or F^- as internal anion (Chandler & Meves, 1965, 1970*a*). A major reason for the loss of selectivity could be the low ionic strength of our perfusion fluid. Chandler & Meves (1965) found that the permeability ratio P_K/P_{Na} of the sodium channel increases from $1/12$ to about $1/6$ when the internal solution is changed from 300 mM-KCl + sucrose to 24 mM-KCl + sucrose (see also Adelman, Cuervo, Dyro & Senft, 1966). Experiments on artificial membranes also indicate a dependence of cation selectivity on ionic strength (Lev & Buzhinsky, 1967).

In conclusion, it seems likely that there is a general loss of selectivity of the Na channel under our experimental conditions which affects both P_{Ca}/P_{Na} and P_{Cs}/P_{Na} . It should, however, be noted that our determinations of the relative permeabilities of the Na channel are based on measurements of the reversal potential of the tetrodotoxin-sensitive current at 10 or 20 msec after the beginning of the clamp pulse. Reliable measurements at shorter times were difficult because of the long lasting capacity transient (see p. 233). The available data suggest that the permeability ratio P_{Ca}/P_{Na} may be smaller than $1/10$ during the first 5 msec after the beginning of the clamp pulse. This suggestion is based on two findings: (a) the different time courses of I_{Na} and I_{Ca} as shown in Fig. 15, (b) the finding that different ratios P_{Ca}/P_{Na} are required to predict I_{Ca} measured at 1–2 msec and I_{Ca} measured at 12 msec from the Na current I_{Na} (Fig. 16). As discussed on pp. 249 and 260, the possibility must be considered that there are two types of tetrodotoxin-sensitive channels under our experimental conditions, fast and slowly inactivating ones, the latter having a lower selectivity than the normal fast inactivating channels.

We are grateful to Professor Sir Alan Hodgkin for his helpful suggestions concerning the analysis of the experiments. We are indebted to Professor W. Ulbricht and Professor E. J. Denton for reading the manuscript. We also wish to thank Dr M. Whitfield for advice concerning the use of ion-selective electrodes. Financial support was provided by the Deutsche Forschungsgemeinschaft.

REFERENCES

- ADELMAN, W. J., JR., CUERVO, L. A., DYRO, F. M. & SENFT, J. P. (1966). Ionic conductances in internally perfused squid axons. *Fedn Proc.* **25**, 570.
- ADELMAN, W. J., JR., DYRO, F. M. & SENFT, J. (1965). Long duration responses obtained from internally perfused axons. *J. gen. Physiol.* **48**, part 2, 1-9.
- ADELMAN, W. J., JR. & SENFT, J. P. (1966). Voltage clamp studies on the effect of internal cesium ion on sodium and potassium currents in the squid giant axon. *J. gen. Physiol.* **50**, 279-293.
- ADELMAN, W. J., JR. & SENFT, J. P. (1970). Prolonged Na currents in perfused squid axons have multiple time constants of inactivation and are not carried through the K conductance. *Biophys. Soc. 14th Ann. Meet.* Abstr. 184a.
- ADELMAN, W. J. & TAYLOR, R. E. (1961). Leakage current rectification in the squid giant axon. *Nature, Lond.* **190**, 883-885.
- BAKER, P. F., HODGKIN, A. L. & MEVES, H. (1964). The effect of diluting the internal solution on the electrical properties of a perfused giant axon. *J. Physiol.* **170**, 541-560.
- BAKER, P. F., HODGKIN, A. L. & RIDGWAY, E. B. (1971). Depolarization and calcium entry in squid giant axons. *J. Physiol.* **218**, 709-755.
- BAKER, P. F., HODGKIN, A. L. & SHAW, T. I. (1962). Replacement of the axoplasm of giant nerve fibres with artificial solutions. *J. Physiol.* **164**, 330-354.
- BATES, R. G. & ALFENAAR, M. (1969). Activity standards for ion-selective electrodes. In *Ion-selective Electrodes*, ed. DURST, R. A., Nat. Bur. Stand. Spec. Publ. **314**, pp. 191-214.
- BEZANILLA, F., ROJAS, E. & TAYLOR, R. E. (1970). Sodium and potassium conductance changes during a membrane action potential. *J. Physiol.* **211**, 729-751.
- BLAUSTEIN, M. P. & GOLDMAN, D. E. (1968). The action of certain polyvalent cations on the voltage-clamped lobster axon. *J. gen. Physiol.* **51**, 279-291.
- CHANDLER, W. K., HODGKIN, A. L. & MEVES, H. (1965). The effect of changing the internal solution on sodium inactivation and related phenomena in giant axons. *J. Physiol.* **180**, 821-836.
- CHANDLER, W. K. & MEVES, H. (1965). Voltage clamp experiments on internally perfused giant axons. *J. Physiol.* **180**, 788-820.
- CHANDLER, W. K. & MEVES, H. (1970a). Sodium and potassium currents in squid axons perfused with fluoride solutions. *J. Physiol.* **211**, 623-652.
- CHANDLER, W. K. & MEVES, H. (1970b). Rate constants associated with changes in sodium conductance in axons perfused with sodium fluoride. *J. Physiol.* **211**, 679-705.
- CHANDLER, W. K. & MEVES, H. (1970c). Slow changes in membrane permeability and long-lasting action potentials in axons perfused with fluoride solutions. *J. Physiol.* **211**, 707-728.
- EHRENSTEIN, G. & FISHMAN, H. M. (1971). Evidence against hydrogen-calcium competition model for activation of electrically excitable membranes. *Nature, New Biol.* **233**, 16-17.
- FALK, G. & LANDA, J. F. (1960). Prolonged response of skeletal muscle in the absence of penetrating anions. *Am. J. Physiol.* **198**, 289-299.
- FATT, P. & GINSBORG, B. L. (1958). The ionic requirements for the production of action potentials in crustacean muscle fibres. *J. Physiol.* **142**, 516-543.
- FRANKENHAEUSER, B. (1960). Sodium permeability in toad nerve and in squid nerve. *J. Physiol.* **152**, 159-166.
- FRANKENHAEUSER, B. & HODGKIN, A. L. (1957). The action of calcium on the electrical properties of squid axons. *J. Physiol.* **137**, 218-244.

- GOLDMAN, D. E. (1943). Potential, impedance, and rectification in membranes. *J. gen. Physiol.* **27**, 37-60.
- HAGIWARA, S., CHICHIBU, S. & NAKA, K. I. (1964). The effects of various ions on resting and spike potentials of barnacle muscle fibers. *J. gen. Physiol.* **48**, 163-179.
- HILLE, B. (1968). Charges and potentials at the nerve surface. Divalent ions and pH. *J. gen. Physiol.* **51**, 221-236.
- HODGKIN, A. L. & HUXLEY, A. F. (1952*a*). Currents carried by sodium and potassium ions through the membrane of the giant axon of *Loligo*. *J. Physiol.* **116**, 449-472.
- HODGKIN, A. L. & HUXLEY, A. F. (1952*b*). A quantitative description of membrane current and its application to conduction and excitation in nerve. *J. Physiol.* **117**, 500-544.
- HODGKIN, A. L., HUXLEY, A. F. & KATZ, B. (1952). Measurement of current-voltage relations in the membrane of the giant axon of *Loligo*. *J. Physiol.* **116**, 424-448.
- HODGKIN, A. L. & KATZ, B. (1949). The effect of sodium ions on the electrical activity of the giant axon of the squid. *J. Physiol.* **108**, 37-77.
- HODGKIN, A. L. & KEYNES, R. D. (1957). Movements of labelled calcium in squid giant axons. *J. Physiol.* **138**, 253-281.
- LEV, A. A. & BUZHINSKY, E. P. (1967). Cation specificity of the model bimolecular phospholipid membranes with incorporated valinomycin. *Tsitologiya* **9**, 102.
- MEVES, H. & VOGEL, W. (1972). Calcium inward currents in internally perfused giant axons of *Loligo forbesi*. *J. Physiol.* **226**, 89-90P.
- MOORE, J. W., NARAHASHI, T., POSTON, R. & ARISPÉ, N. (1970). Leakage currents in squid axon. *Biophys. Soc. 14th Ann. Meet. Abstr.* 180a.
- ROBINSON, R. A. & STOKES, R. H. (1959). *Electrolyte Solutions*, 2nd edn. London: Butterworths.
- SHATKAY, A. (1968). Individual activity of calcium ions in pure solutions of CaCl₂ and in mixtures. *Biophys. J.* **8**, 912-919.
- TAKENAKA, T. & YUMOTO, K. (1969). Time course analysis of cation influxes during the prolonged action potential in perfused squid giant axon. *Proc. Japan Acad.* **45**, 751-756.
- TASAKI, I., LERMAN, L. & WATANABE, A. (1969). Analysis of excitation process in squid giant axons under bi-ionic conditions. *Am. J. Physiol.* **216**, 130-138.
- TASAKI, I., WATANABE, A. & LERMAN, L. (1967). Role of divalent cations in excitation of squid giant axons. *Am. J. Physiol.* **213**, 1465-1474.
- TASAKI, I., WATANABE, A. & SINGER, I. (1966). Excitability of squid giant axons in the absence of univalent cations in the external medium. *Proc. natn. Acad. Sci. U.S.A.* **56**, 1116-1122.
- WATANABE, A., TASAKI, I. & LERMAN, L. (1967*a*). Bi-ionic action potentials in squid giant axons internally perfused with sodium salts. *Proc. natn. Acad. Sci. U.S.A.* **58**, 2246-2252.
- WATANABE, A., TASAKI, I., SINGER, I. & LERMAN, L. (1967*b*). Effects of tetrodotoxin on excitability of squid giant axons in sodium-free media. *Science, N.Y.* **155**, 95-97.